8-2019

Investigation of DSR Test Methods to Determine Binder Low Temperature Properties

Kommidi Santosh
University of Nebraska-Lincoln, santosh.kommidi@gmail.com

Yong-Rak Kim
University of Nebraska-Lincoln, yong-rak.kim@unl.edu

NEBRASKA TRANSPORTATION CENTER

NEBRASKA DEPARTMENT OF TRANSPORTATION

Report SPR-1 (18) M073

Final Report
26-1121-4041-001

Investigation of DSR Test Methods to Determine Binder Low Temperature Properties

Santosh Reddy Kommidi, M.S.
Graduate Research Assistant
Department of Civil Engineering
University of Nebraska-Lincoln

Yong-Rak Kim, Ph.D.
Professor

2019

Nebraska Transportation Center
262 Prem S. Paul Research Center at Whittier School
2200 Vine Street
Lincoln, NE 68583-0851
(402) 472-1993

Investigation of DSR Test Methods to Determine Binder Low Temperature Properties

Santosh Reddy Kommidi, M.S.

Graduate Research Assistant

Department of Civil Engineering

University of Nebraska-Lincoln

Yong-Rak Kim, Ph.D.

Professor

Department of Civil Engineering

University of Nebraska-Lincoln

A Report on Research Sponsored by

Nebraska Department of Transportation

August 2019

Technical Report Documentation Page

1. Report No NDOT: SPR-1 (18) M073 NTC: 26-1121-4041-001	2. Government Accession No.	3. Recipient's Catalog No.	
4. Title and Subtitle Investigation of DSR Test Methods to Determine Binder Low Temperature Properties		5. Report Date August 2019	
		6. Performing Organization Code	
7. Author/s Santosh Reddy Kommidi and Yong-Rak Kim		8. Performing Organization Report No. 26-1121-4041-001	
9. Performing Organization Name and Address Nebraska Transportation Center University of Nebraska-Lincoln (Department of Civil Engineering) 362N WHIT, 2200 Vine St., Lincoln, NE 68583-0856		10. Work Unit No. (TRAIS)	
		11. Contract or Grant No.	
12. Sponsoring Organization Name and Address Nebraska Department of Transportation (NDOT) 1400 Highway 2, PO Box 94759, Lincoln, NE 68509		13. Type of Report and Period Covered 07/01/2017 – 08/15/2019	
		14. Sponsoring Agency Code	
15. Supplementary Notes			
16. Abstract The low temperature rheology of bituminous binders is of great interest because low temperature cracking is one of the primary asphalt pavement failure modes observed in cold-climate places such as Nebraska. Low temperature binder characterization/grading has been primarily conducted using the bending beam rheometer (BBR), while the dynamic shear rheometer (DSR) can alternatively be used to characterize the low temperature properties of binders with the recent advancement of DSR equipment that can cover a wide range of testing temperatures. This study investigates alternative testing-analysis methods using the DSR to determine low temperature asphalt binder properties that have been measured by the BBR. Toward that end, twelve different binders from four sources satisfying three different PG grading criterion common in Nebraska were selected. The binder samples were tested in the frequency domain at temperatures ranging from 60°C to -30°C under PAV-aged conditions using DSR. The 8-mm parallel plate geometry was primarily employed for the testing, while four binders were randomly selected and tested using the 4-mm parallel plate to investigate the influence of geometry on the results. BBR experiments were also performed as a parallel for each binder. Three methods were used to analyze and compare the data from the two different experiments (i.e., DSR and BBR) where each method utilizes a different scheme for converting the frequency domain results to time domain data to compare with the BBR results. The three methods are: (1) Western Research Institute's (WRI) methodology; (2) NCHRP methodology; and (3) UNL's mechanistic approach. It was observed that the DSR testing is quite promising, and sample preparation is crucial to obtain reliable-repeatable results. Moreover, in the proposed UNL's mechanistic approach, it was observed that a single shift factor for creep compliance may account for different testing conditions, differences in physical hardening and temperature-dependent effects. The approach was then extended to seven additional binders to further examine its feasibility, and it was observed that the predictions from the proposed approach match well with the experimental values.			
17. Key Words Low temperature property of binder; Performance grading; Dynamic shear rheometer; Bending beam rheometer; Mechanistic conversion	18. Distribution Statement		
19. Security Classification (of this report) Unclassified	20. Security Classification (this page) Unclassified	21. No. Of Pages 77	22. Price

Table of Contents

List of Figures

List of Tables

Acknowledgements

The authors would like to thank the Nebraska Department of Transportation (NDOT) for the financial support needed to complete this study. In particular, the authors thank the NDOT Technical Advisory Committee (TAC) for their technical support and their invaluable discussion and comments.

Disclaimer

The contents of this report reflect the views of the authors, who are responsible for the facts and the accuracy of the information presented herein. This document is disseminated under the sponsorship of the U.S. Department of Transportation's University Transportation Centers Program, in the interest of information exchange. The U.S. Government assumes no liability for the contents or use thereof.

Abstract

The low temperature rheology of bituminous binders is of great interest because low temperature cracking is one of the primary asphalt pavement failure modes observed in cold-climate places such as Nebraska. Low temperature binder characterization/grading has been primarily conducted using the bending beam rheometer (BBR), while the dynamic shear rheometer (DSR) can alternatively be used to characterize the low temperature properties of binders with the recent advancement of DSR equipment that can cover a wide range of testing temperatures. This study investigates alternative testing-analysis methods using the DSR to determine low temperature asphalt binder properties that have been measured by the BBR. Toward that end, twelve different binders from four sources satisfying three different PG grading criterion common in Nebraska were selected. The binder samples were tested in the frequency domain at temperatures ranging from 60°C to -30°C under PAV-aged conditions using DSR. The 8-mm parallel plate geometry was primarily employed for the testing, while four binders were randomly selected and tested using the 4-mm parallel plate to investigate the influence of geometry on the results. BBR experiments were also performed as a parallel for each binder. Three methods were used to analyze and compare the data from the two different experiments (i.e., DSR and BBR) where each method utilizes a different scheme for converting the frequency domain results to time domain data to compare with the BBR results. The three methods are: (1) Western Research Institute's (WRI) methodology; (2) NCHRP methodology; and (3) UNL's mechanistic approach. It was observed that the DSR testing is quite promising, and sample preparation is crucial to obtain reliable-repeatable results. Moreover, in the proposed UNL's mechanistic approach, it was observed that a single shift factor for creep compliance may account for different testing conditions, differences in physical hardening and temperature-dependent effects. The approach was then extended to seven additional binders to further examine its feasibility, and it was observed that the predictions from the proposed approach match well with the experimental values.

Chapter 1. Introduction

The low-temperature rheology of bituminous binders is of great interest because low-temperature cracking is one of the primary asphalt pavement failure modes observed in cold-climate regions such as Nebraska. Moreover, binder properties have been found to mainly determine the thermal cracking performance of asphalt pavements, other asphalt mixture properties being of secondary importance (*1*). Low-temperature cracking typically occurs during extreme low-temperature weather, usually within a few years after pavement construction. This failure mode is visible in the asphalt pavement as transverse cracks that are caused by the binder's inability to deform to reduce stress. When the stresses exceed the asphalt binder's strength, transverse cracks appear. To reduce the frequency of low-temperature cracking failure, the strength or stress relaxation ability of the binder must be increased.

The dynamic shear rheometer (DSR) is the critical apparatus used in the Superpave performance-graded (PG) binder system for high and intermediate temperature, while the bending beam rheometer (BBR) is a core equipment for low temperature. During the Strategic Highway Research Program (SHRP) (*2*), DSR with parallel plate geometry was considered for the low temperature PG system, but it was not selected because it was recognized that DSR measurements at temperatures below about 5°C produced instrument compliance errors in the dynamic responses when the typical thin film binder geometry was used. Thus, SHRP developed the BBR to measure the low temperature rheological properties of asphalt binder (AASHTO T 313). A literature review reveals that in the 1990s and 2000s numerous articles were published concerning the low-temperature rheology of bitumen (*3-11*). However, the results of the studies where DSR has been employed to measure bitumen's low temperature characteristics are subject to criticism. This is because in these investigations, the data measured with 8 mm parallel plate geometry have been reported without accurate instrument compliance correction. Consequently, the reliability of these test results is rather questionable. The limiting temperature of about 5°C for DSR parallel plate measurements due to instrument compliance has been resolved by measuring the instrument compliance and performing appropriate corrections to the data. According to the studies (*12-15*) performed by Western Research Institute's researchers, DSR measurements can now be made to as low as -40°C.

Although the BBR method has been an official approach to measure low temperature properties, it has several operational drawbacks. The BBR requires a long time (approximately 3 hours) to fabricate specimens and conduct testing, and it requires large amounts of binder (approximately 15 grams) to fabricate each testing specimen which clearly limits testing of binders obtained from field sections. Field studies to monitor pavement performance over time are becoming ever more important. However, it is very labor-intensive and time-consuming to extract large amounts of binder from an existing asphalt pavement for BBR testing. To minimize this effort, a binder test that uses only small amounts of material would be great. Another drawback of the BBR method is that it is not fundamentally sound to evaluate low temperature cracking potential of binders because it only measures binder stiffness (i.e., creep stiffness and the rate of relaxation) not binder fracture. A clear benefit is expected if the current BBR method for low temperature evaluation of binders can be supplemented (or replaced) by an alternative method to advance efficiency, accuracy of binder grading-evaluation program. In particular, if the method is based on the DSR testing, single equipment would be necessary to examine binders for an entire temperature range, which can reduce testing time and costs significantly.

1.1 Research Objective

The objective of this research is to seek an alternative testing or analysis method using the DSR to determine low temperature asphalt binder properties that is currently being measured by the BBR. More specifically the goal is to develop a DSR testing and/or analysis method and resulting material parameters to supplement (or potentially replace) the BBR approach, which will be based on scientific comparison/correlation of test results between the two methods. Multiple binders used in Nebraska were tested to reach general conclusions. It is expected that the alternative testing or analysis method can serve as a useful tool for screening binders before performing entire BBR tests, or possibly replace the current BBR testing protocol for low temperature examination of binders. It is expected that one equipment (i.e., DSR) would characterize entire binder properties in all temperatures, which will clearly save costs and time to conduct quality assurance testing of binders. Ultimately, this research will contribute to a more engineered and economical implementation of paving materials in Nebraska by providing crucial information and scientific insights.

1.2 Research Methodology

Figure 1.1 shows a schematic of the methodology adopted in this study. First, the low temperature rheological behavior for each binder was obtained using the DSR with 8mm and 4mm parallel plates. For each binder, material responses that are dependent on temperature and loading frequency are identified by developing linear viscoelastic master curves of oscillatory responses such as dynamic modulus (|G*|), storage modulus (G'), loss modulus (G'') and phase angle (δ). Later, the theory of linear viscoelasticity was used to represent the binder response and to obtain viscoelastic material parameters by fitting the model response to the master curves.

This study attempts to seek alternative testing-analysis methods using the DSR to determine low temperature asphalt binder properties that have been measured by the BBR. Toward that end, twelve different binders from four sources satisfying three different PG grading criterion common in Nebraska were selected. The binder samples were tested in the frequency domain at temperatures ranging from 60°C to -30°C under PAV-aged conditions using DSR. BBR experiments were also performed as a parallel for each binder. Three methods were used to analyze and compare the data from the two different experiments (i.e., DSR and BBR) where each method utilizes a different scheme for converting the frequency domain results to time domain data to compare with the BBR results. The three methods are: (1) Western Research Institute's (WRI) methodology; (2) NCHRP methodology; and (3) UNL's mechanistic approach.

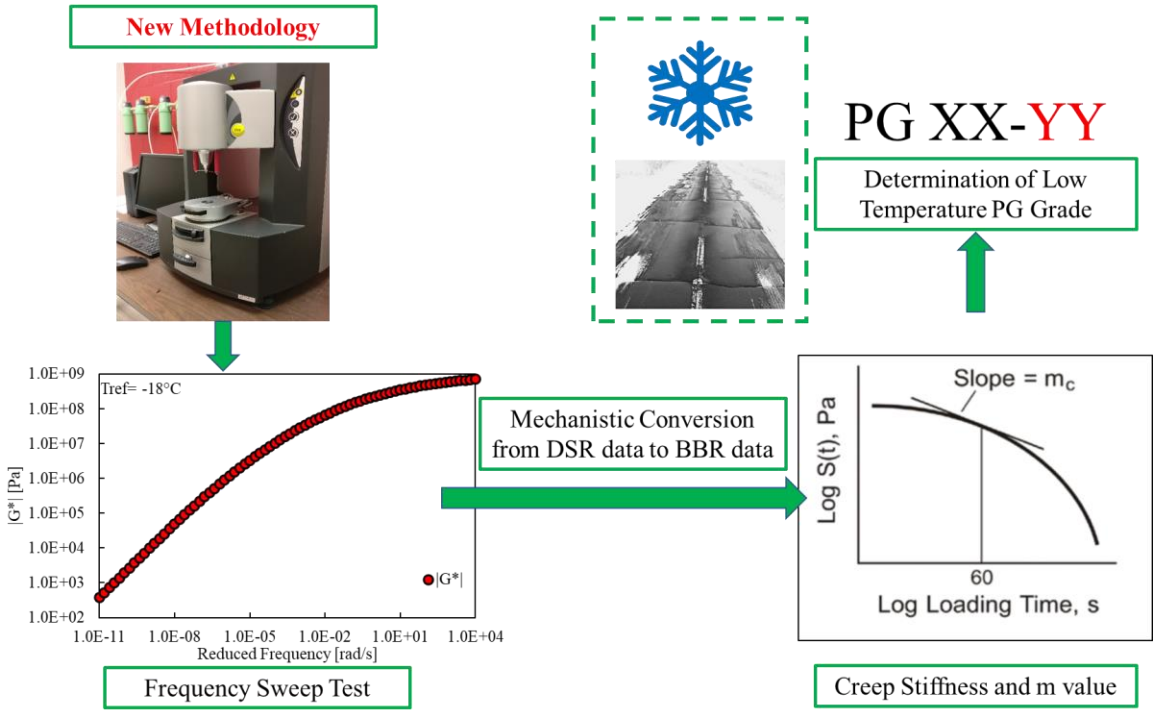

Figure 1.1 Research methodology for binder low temperature characterization.

1.3 Organization of Report

This report is organized into five chapters. After this introduction, chapter 2 describes a brief literature review that summarizes relevant studies. Chapter 3 presents materials (i.e., binders) used in this study and sample fabrication of the binders for laboratory testing (i.e., BBR and DSR). Test results and analyses of results are presented in Chapter 4. Significant findings and conclusive outcomes including future studies recommended are summarized in Chapter 5: Summary and Conclusions.

Chapter 2. Literature Review

In cold places such as Nebraska that experience very low temperature over prolonged periods of time and experience multiple freeze-thaw cycles, the primary form of pavement distress is low temperature transverse cracks. Such cracks can appear over a certain period of years after pavement construction. The development of such cracks can be mainly attributed to factors such as pavement material properties, structure of the pavement, and the environment (*1*). There are several other factors that can trigger such cracks as well (*16, 17*), but from the perspective of the material, the main cause of low temperature cracks can be attributed to development of critical thermal stresses within the binder phase. Over the last few years, the use of reclaimed asphalt pavements has increased considerably, which has thereby increased the pavement's susceptibility to early low temperature cracks (*18*). Over the last three decades, considerable insight into the low temperature behavior of asphalt binder has been gained (*19*). Low temperature binder characterization can be broadly classified into two categories based on the type of type of investigation and approach:

- Stiffness-based approach: this relies on methods or experiments designed to capture the linear viscoelastic material properties of the binder.
- Fracture-based approach: this relies on methods or experiments designed to capture the linear elastic/plastic/viscoelastic/viscoelastic-viscoplastic fracture properties of asphalt binder.

One of the earliest and most comprehensive characterizations of the asphalt binder rheological properties was conducted during the 1900's as part of the Strategic Highway Research Program (SHRP) (*2*). This program developed a testing protocol based on a three-point bending test on a binder beam sample using the bending beam rheometer (BBR) to assess the low temperature response of a given binder. Based on subsequent research efforts, limits were placed on the creep stiffness $S(t)$ and slope of log ($S(t)$) when plotted against log (t) measured at time t = 60 s. The critical low temperature was identified to be 10°C lower than the temperature where these limits ($S(t) \leq 300$ MPa and $m(t) \geq 0.3$) were reached. A supplementary fracture-based test, the Direct Tension Test (DTT) (*20*) was introduced as part of the original PG grading but it was soon considered to be optional and finally stopped being used due to issues with poor

repeatability. As is the case with most fracture related tests performed on pure asphalt binders, it was observed that repeatability issues with the DTT test were specific to the selected binder and sample preparation technique.

2.1 Drawback of Performance Grading (PG)

The applicability of the Time Temperature Superposition Principle (TTSP) to evaluate the stiffness- $S(t=60s)$ and slope-$m(t=60s)$ parameters is questionable (*21, 22*). There are several parameters that the current PG grading criterion does not account for; some of these factors are the source of the binder and influence of modification (polymer, nano-filler, reclaimed asphalt binder, effect of rejuvenators, warm-mix additives). Current PG grading is not specific to a given binder nor does it include temperature and time-dependent behavior over a wide range of low temperatures. Use of high Reclaimed Asphalt Pavement (RAP) increases the aged asphalt content within the pavement and hence warrants a new technique/methodology for analyzing the low temperature performance of the modified binders. The current PG grading requires at least 15 to 30 grams of binder to obtain the critical low temperature grade of the binder that prohibits its use as a monitoring tool for evaluating the performance of pavement in terms of binder properties.

Nonetheless, the NCHRP program has been successful in terms of its application, since PG grading has been in use for nearly four decades. The NCHRP program has also identified several key research areas such physical hardening effects that were more severe in certain binders as compared to other binders, revealing a need for a fracture-based approach for evaluating the fracture properties of a binder.

2.2 Binder Fracture Based Tests

The motivation for researchers to consider fracture-based characterization of the binder is mainly due to the fact that current PG grading is based on the principles of linear viscoelastic properties of the binder. The belief is that PG grading cannot account for the complex cracking phenomenon that occurs in pavements (*23*). Listed below are some of the fracture-based testing methods used for asphalt binders. A detailed description of each test method is not presented, as the current scope of the study does not include fracture of binder.

- Direct Tensile Test (DTT)

- Single-Edged Notched Beam (SENB) (*24-27*) or the BBR-SENB Test (*28*)
- Double-Edged Notched Tension Test (DENT) (*29-33*)
- Asphalt Binder Cracking Device (ABCD) Test (*34-36*)
- Evaluation of Cracking using Acoustic Emission (*16, 37*)

The major limitations that can be associated with the fracture-based tests for use as a specification type for binder is listed below:

- The loads applied in such experiments are small in the range of 5-20 N for unmodified and modified binders and 15-30 N for RAP modified binders. Although, this may not be a great challenge with current technological advancements in capturing low levels of load, precise control of sample preparation (e.g., notch size and sample thickness) and testing necessary to generate repeatable results.
- Repeatability is often an issue with fracture-based experiments, which further depends on the type and source of binder and sample fabrication methods.
- Selection of the temperature for fracture testing can be quite tricky when using an ungraded binder due to ductile to the brittle behavior of binder at temperatures closer to the glass transition temperature (T_g) which requires multiple experiments to be conducted at several temperatures.
- Post peak behavior in certain fracture tests such as the BBR-SENB is too short for a comprehensive analysis of fracture resistance properties of binder due to uncontrolled crack opening displacements.
- Single event tests such as the Fraas Breaking Point and ABCD cannot capture thermal history dependent behavior of the asphalt binder more comprehensively.

2.3 Physical Hardening of Binder al Low Temperatures

Two important phenomenon that can significantly affect the low temperature behavior of binders is the glass transition temperature (T_g) and significant physical hardening of binder at temperatures closer to T_g (*2, 38*). Several researchers have investigated the influence of physical hardening on the PG grading criterion (*17, 29, 38, 39*). Physical hardening effects can be critical to certain binders with high wax content and is related to the free volume changes that occur at temperatures close to the T_g. When the binder temperature is close to T_g, there is a transition region where the effects of physical hardening can be critical. This transition region is due to the

presence of different molecular fractions within the asphalt binder. This transition region can be broad for binders (*40*) and can be an important factor that needs to be considered, since the binder can encounter these temperatures during the service of the pavement. Measurable effects of physical hardening occur in the vicinity of the glass transition temperature. Since the objective of the current investigation is to develop a robust and fast methodology for low temperature characterization using DSR, the physical hardening effects have been considered a different approach detailed in later chapters. Interested readers are directed to the work by Laukkanen et al. (*41*) who investigated the physical aging in binders using the small diameter plate rheology with the DSR. Their method for characterizing the physical hardening, although quite comprehensive can take days for a single binder and was hence avoided for the current study.

2.4 Low Temperature Characterization of Binder Based on Rheology

Due to increased usage of reclaimed asphalt binder (RAB) and various other additives (e.g., warm-mix additives, emulsions, crack sealants, nano-fillers) it can be difficult to conduct a forensic analysis or performance evaluation of the binder at low temperatures. Such an investigation would require extraction of a large amount of binder for conducting the current BBR low temperature PG grading. Considering the difficulty associated with the current PG grading system for field monitoring purposes, Sui et al. (*12*, *13*) developed a new technique for low temperature characterization of binder using the dynamic shear rheometer (DSR) 4-mm parallel plate geometry. After evaluating several key factors such as instrument compliance correction, different plate geometries and repeatability, Sui et al. concluded that evaluation of low temperature performance of the binder using DSR is more reliable and faster than the current low temperature PG grading. In an extension of the above study, Farrar et al. (*14*) developed a probable specification test for low temperature grading using the DSR. They observed linear correlations between the DSR obtained relaxation modulus $G(t{=}60s)$, its slope $m_{G(t)}(t = 60s)$ and the corresponding BBR stiffness $S(t = 60s)$ and its slope $m_{S(t)}(t = 60s)$ at low PG+10°C temperature. Based on the correlations they established limiting relaxation modulus $G(t = 60s)$ and slope $m_{G(t)}(t = 60s)$ criterion. A similar investigation was carried out by Xiaohu et al. (*42*) using the DSR and 4-mm parallel plate geometry, in which they compared the dynamic modulus ($|G^*|$) and phase angle (δ) at certain frequencies to the BBR creep stiffness $S(t = 60s)$ and $m(t = 60s)$ measured at the binder low temperature PG+10°C. They concluded that critical low

temperature grades predicted by the DSR were lower than those predicted by the BBR tests, which was attributed to wax content within the binder system. In another study, Laukkanen et al. (*43, 44*) investigated the use of small diameter parallel plate (SDPP) rheometer and necessary compliance correction to evaluate the low temperature behavior of binder. They observed that binder belongs to the class of complex glass forming liquids and that by using small diameter plates, DSR tests can be used to effectively characterize the low temperature behavior of the binder. Laukkanen et al. (*45*) examined the influence of SBS polymer on the low temperature rheological behavior of two binders using 4-mm DSR. They observed linear correlations between DSR dynamic modulus ($|G^*|$) and BBR stiffness $S(t)$ for a continuous SBS rich network. Deviations from linearity were attributed to poor compatibility between the polymer and base binder. They concluded that the rheological response of SBS polymer-modified binders at low temperatures can be thermo-rheologically complex.

In another study Carret et al. (*46*) investigated two sets of binder samples using DSR at low temperatures. The first set of four binder samples were tested using solid bars in torsion and the second set of two binder samples were tested using 4-mm parallel plate geometry. The same binder samples were tested using the BBR at different temperatures (-30°C to -6°C at every 6°C increment). Linear viscoelastic models were utilized to represent the material response measured using DSR and obtained the creep stiffness at the corresponding BBR test temperatures. They compared the DSR stiffness to the BBR stiffness and it was concluded that horizontal and vertical shift factors were needed to match the two results. The shift factors were necessary to account for differences in conditioning times, physical hardening and cooling media used for the DSR and BBR experiments. Recently, Riccardi et al. (*47*) investigated the effects of different cooling media (air and ethanol) on the mechanical response of three binders tested using the BBR. It was observed that use of air as the cooling medium resulted in higher stiffness and lower relaxation capabilities as compared to the test response in ethanol for the same binder.

Based on the above literature review it can be concluded that there is a quite appealing need to explore a DSR-based method for characterizing the low temperature properties of binders. Development of such a method will produce cost savings, enhance work efficiency and wider application of the technique to field materials using a single equipment.

Chapter 3. Materials, Sample Fabrication and Testing

For the current investigation, 12 binders from four different sources that satisfied different low temperature PG specification were selected. The selected binders were common to the state of Nebraska. In order to include variation in the analysis, binders satisfying three different low temperature grades (i.e., PG 58-34, PG 64-28 and PG 64-22) were selected from each binder source as shown in Table 3.1.

All the binders were aged using RTFOT and PAV aging tests to simulate short-term and long-term aging. In the current investigation, all the experiments (BBR and DSR) were performed on the PAV-aged material.

Table 3.1 Source and PG Grade of the Binders Selected

Binder Source	Performance Grade
Jebro (J)	PG 58-34
Flint Hills (F)	PG 64-28
Western State Asphalts (W)	PG 64-22
Suncor (S)	

3.1 Sample Fabrication

3.1.1 Bending Beam Rheometer (BBR)

To prepare the BBR samples, approximately 25 g of binder was heated in a small container till the binder could flow easily. Then, the heated binder was poured into the mold as shown in Figure 3.1 and was then allowed to cool for 30 min. Once the binder samples cooled to room temperature, excess binder on the top of the mold was carefully trimmed to leave a smooth surface at the top followed by refrigeration for 20 min. Next, the metal components were carefully demolded to obtain a solid beam sample as shown in Figure 3.1. The beam sample dimensions (length x width x depth) were 125 mm x 12.5 mm x 6.5 mm. The entire BBR sample preparation was performed according to the method described in ASTM 6648-08 (2016).

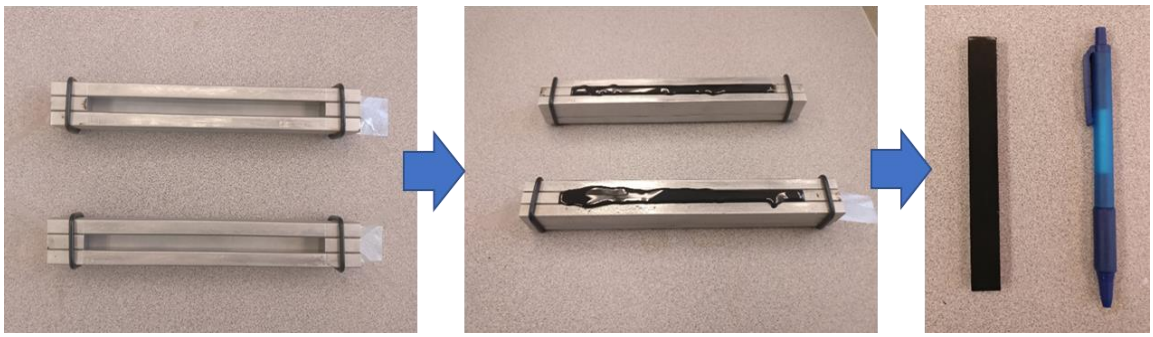

Figure 3.1 BBR Sample preparation scheme.

3.1.2 Dynamic Shear Rheometer (DSR)

Sample preparation for the DSR tests using either the 8-mm or the 4-mm parallel plate is relatively much easier, simpler and less time consuming as compared to the BBR sample preparation. This is one of the major reasons why the low temperature characterization of binder using the DSR has received more attention in recent years as compared to BBR. For the DSR binder samples, the binder was heated until the sample was soft enough to flow and was then poured into the corresponding molds as shown in Figure 3.2.

(a) (b)

Figure 3.2 (a) 8-mm DSR mold (b) 4-mm DSR mold.

Precise preparation of the DSR samples is critical for obtaining representative and repeatable results. Since the DSR tests were also conducted at temperatures below freezing, significantly large error in estimating the material properties can occur if the sample is incorrectly placed or trimmed. Figure 3.3 exemplifies sample placement and trimming process for a 4-mm parallel plate sample. Analysis on the effects of improper DSR sample preparation between the plates is discussed in detail in chapter 4.

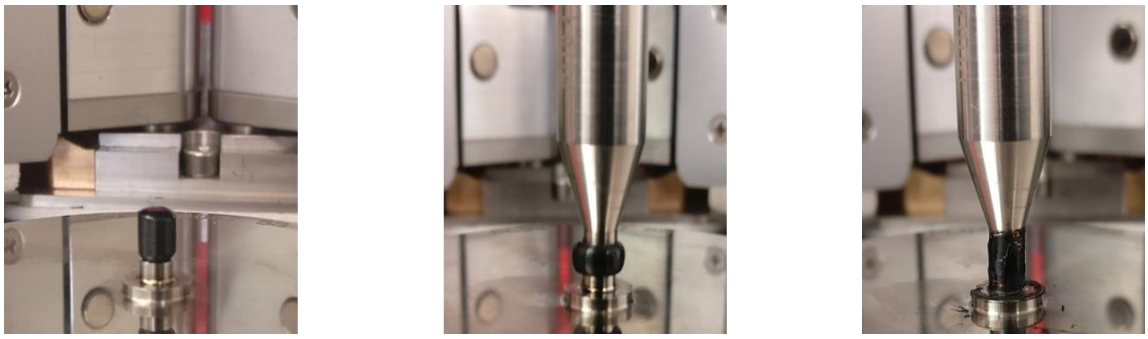

Figure 3.3 4-mm sample placement and trimming for testing using the DSR.

Since the current investigation mainly focused on the low temperature properties of binder, two specific tests were performed on each of the binder samples to obtain their material properties; namely, BBR and DSR. The section below describes the BBR test methodology and then DSR testing scheme utilized for obtaining the low temperature rheological response over a wide range of temperatures.

3.2 Testing Scheme

3.2.1 Three-point Bending Beam Test (BBR)

Testing of the 12 BBR samples was conducted using the ATS Bending Beam Rheometer, as shown in Figure 3.4. The beam samples were subjected to a three-point bending test with the load applied at the mid-span of the beam. The temperature control was exerted by an external temperature control unit and a uniform temperature field was achieved using a cooling medium within the chamber. The current investigation used a cooling medium consisting of a blend of 50 % by volume ethanol and 50% by volume 2-propanol. Several concerns have been raised *(46, 47*) regarding the influence of cooling medium such as using only ethanol, on the properties obtained using the BBR tests. It was observed that the chemical influence of this blend (50 % by volume ethanol + 50% by volume 2-propanol) on the binder properties was negligible.

In the three-point bending test, a contact load of 35 ± 10 mN followed by a constant test load of 980 ± 50 mN was applied at the mid span of the beam. The time dependent deflection at the bottom mid-span was measured during the application of the test load. The beam stiffness, $S(t)$ as a function of time was estimated using the Equation 3.1.

$$S(t) = \frac{PL^3}{4bh^3\Delta(t)} \tag{3.1}$$

where P is the test load, L is the span length, b and h are the beam width and depth, respectively and $\Delta(t)$ is the time-dependent deflection measured using BBR. The NCHRP PG low temperature criterion measured at a temperature T+10 °C are, stiffness, $S(t{=}60\text{s}) \leq 300$ MPa and slope, $m(t{=}60\text{s}) \geq 0.3$, where $m(t)$ is the slope of $\log(S(t))$ vs $\log(t)$ curve.

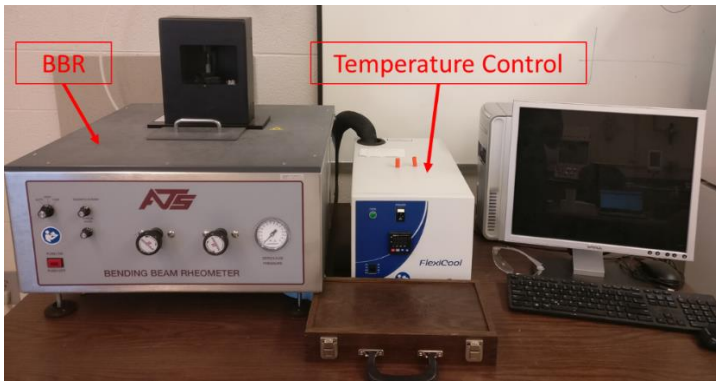

(a)

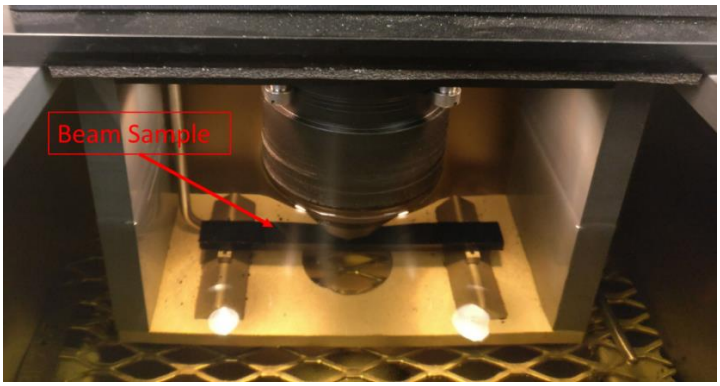

(b)

Figure 3.4 (a) Bending Beam Rheometer with cooling unit (b) BBR beam sample loaded on the testing frame surrounded by the cooling media 50 % by volume propanol and 50 % volume ethanol.

3.2.2 Frequency Sweep (DSR)

The low temperature material response of each binder was evaluated by performing frequency sweep tests to obtain the non-destructive material dependent linear viscoelastic properties. The frequency sweep data were later used to obtain the master curve at a specific reference temperature using time-temperature superposition principle. Selection of the reference temperature was based on the low temperature PG grade of the binder sample. For instance, if the binder was graded as PG 64-34, then the reference temperature (T_{ref}) was selected as 10°C higher than the graded low temperature, which in this case was -24 °C. Each of the 12 binder samples were subjected to frequency sweep tests at temperatures ranging from 64 °C to -30 °C. At each temperature, the frequency was increased from 0.628 rad/s to 80 rad/s; the strain amplitude selected for the frequency sweep test at the individual temperature is shown in Table 3.2. As the temperature decreased the strain amplitude was reduced, which maintained the sample response to be within the linear viscoelastic regime.

Table 3.2 Strain Chosen for Corresponding Temperature for Linear Viscoelastic Behavior

Temperature	**8-mm Plate**		**4-mm Plate**	**Strain**
	Trial-1	**Trial-2**	**Trial-1**	
64 ºC to 45 ºC	✓	✓	×	0.1 %
35 ºC to 10 ºC	✓	✓	×	0.01 %
0 ºC to -30 ºC	✓	✓	✓	0.001 %

Figure 3.5 shows an example of the frequency sweep test conducted on sample J64-28 (i.e., PG 64-28 from Jebro) at temperatures ranging from 64 °C to -30 °C and the constructed master curves for complex shear modulus ($|G^*|$), storage modulus (G'), loss modulus (G'') and phase angle (δ) at the reference temperature of -18 °C. Figure 3.5(a) shows the frequency sweep results at individual temperatures. After generating the master curves the data were smoothed using a polynomial function in the logarithmic scales. The smoothed master curves are shown in Figure 3.5(b). Smoothing was only restricted to the limits of the experimental data without any extrapolation such that no additional data points were added after the smoothing process.

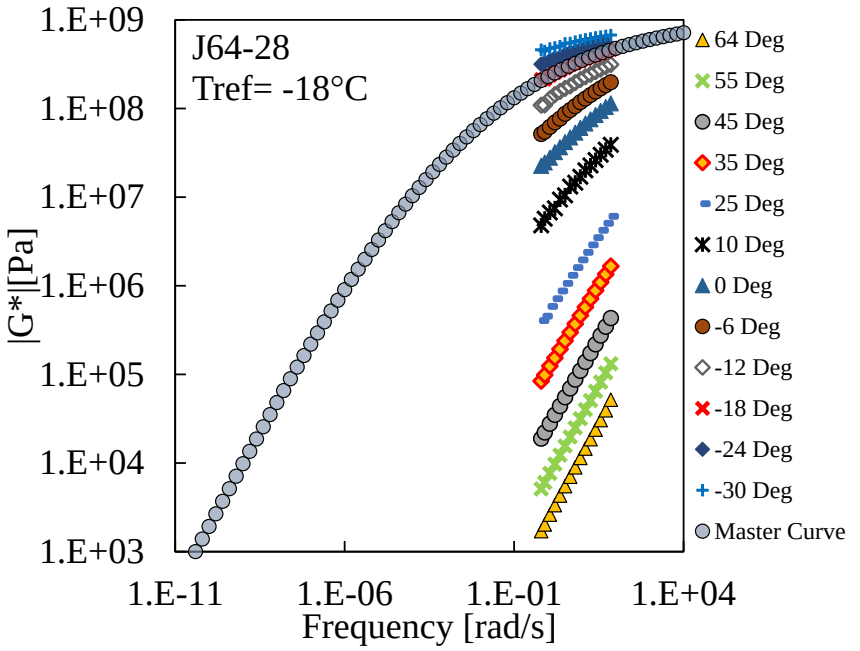

(a)

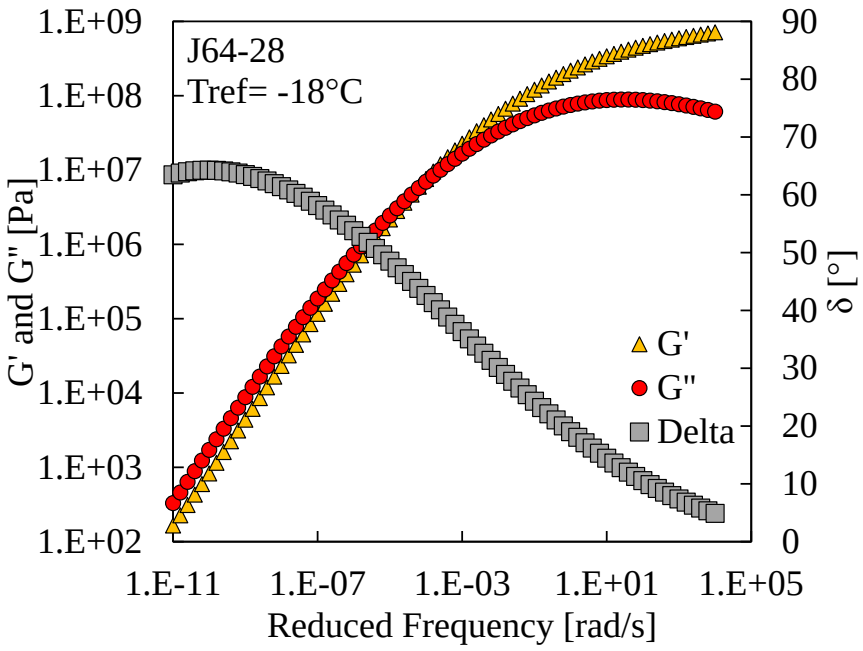

(b)

Figure 3.5 (a) |*G**| data at different temperatures and master curve for |*G**|, (b) master curves for *G'*,*G''* and δ for sample J64-28.

While performing the frequency sweep experiments using the DSR there are several key factors that need to be considered when performing the tests at temperatures below 0 °C. These factors play a critical role in obtaining the material properties or response at freezing temperatures. The factors are described below:

1. Sample Preparation and Test Geometry

   Precise control over the sample preparation and test geometry after trimming the sample is necessary in order to obtain repeatable results. Since the testing conditions and temperature for the DSR can be below 0°C, significant differences from the actual response is possible if there is excess or less sample between the plates.

2. Normal Force/Gap Control When Testing Below 0 °C:

   During torsion testing at low temperatures, the binder can shrink due to increase in thermal contraction which cause substantial negative normal force on the upper parallel plate. In order to avoid such additional thermal stresses a normal-force controlled gap variation between the parallel plates must be allowed during testing at temperatures below 0 °C. Normally the gap between the plates is fixed to 2 mm and 1.75 mm for 8-mm and 4-mm parallel plates. Hence, this sample thickness can vary during the gap-controlled experiments to keep the normal force on the top plate at minimal levels that allow the thermal stresses to relax completely while testing.

3. Compliance Correction:

   When a given binder sample is tested at temperatures close to the T_g, the binder stiffness increases considerably and is comparable to that of the plates and motor, which results in distortion of parallel plates and the instrument motor (*48-50*). In such situations, the expected material response to loading is not from the binder sample alone due to the contribution of deformation from the plates and motor. Hence suitable compliance corrections to the data are necessary when testing a low temperature. Sui et al. (*13*) and Laukkanen et al. (*43*) demonstrated how to manually correct the data by considering the instrument correction for different plate diameter and materials. Since considerable research has been devoted to this issue, most of the current DSR have incorporated for

automatic data correction through the software that is used to control the device during testing at low temperatures.

4. Cooling Media:

   The effect of cooling media on the rheological properties of the binder using the DSR is not well documented and needs to be further investigated. In the current investigation air was used as the cooling medium for both the 8-mm and 4-mm parallel plate geometries. Use of an inert gas environment, such as nitrogen can be used to avoid buildup of ice near and around the binder sample.

All 12 binder samples were tested using the 8-mm parallel plate geometry and only a few selected samples were tested using the 4 mm parallel plate geometry to check for the influence of instrument compliance at low temperature, the results of which are discussed in detail in Chapter 4. The sample thickness for the 8-mm and 4-mm parallel plates were maintained at 2 mm and 1.75 mm, respectively. Table 3.3 shows the list of binder samples tested using the 8-mm parallel plate and the Table 3.4 shows the samples tested using 4-mm parallel plate geometry.

Table 3.3 Samples Tested to Obtain Frequency Sweep Results Using 8-mm Parallel Plate

Source	Grade	8-mm Plate	
		Trial-1	Trial-2
Suncor	PG 58-34	✓	✓
	PG 64-28	✓	✓
	PG 64-22	✓	×
Western State Asphalt	PG 58-34	✓	✓
	PG 64-28	✓	×
	PG 64-22	✓	✓
Flint Hills	PG 58-34	✓	✓
	PG 64-28	✓	×
	PG 64-22	✓	✓
Jebro	PG 58-34	✓	✓
	PG 64-28	✓	✓
	PG 64-22	✓	✓

Table 3.4 Samples Tested to Obtain Frequency Sweep Results Using 4-mm Parallel Plate

Source	Grade
Suncor	PG 58-34
Western State Asphalt	PG 64-22
Jebro	PG 64-28, PG 58-34

Chapter 4. Results and Discussion

To investigate the influence of low freezing temperatures on the mechanical response of the binder, two types of tests were performed on the three PG grade binder samples selected in the current investigation. The low temperature tests on the binder were performed using the BBR and DSR.

4.1 BBR Test Results

Bending beam tests were performed on each of the 12 PAV-aged binder samples described in Table 3.1. The tests were performed in accordance to the ASTM 6648-08 (2016) standard to maintain consistency. Details of the sample preparation method and experimental data collection is described in Chapter 3. Since the binder samples were already assigned a PG grade from the manufacturer, low temperature grading of the binder samples was not performed in our study instead, BBR tests were conducted at a reference temperature based on the manufacturer's grading. For example, if the binder J58-34 was selected, the reference temperature for the BBR test was low PG +10 °C, in this case it would be T_{ref} = -24°C. For each binder, three replicates were performed at the reference temperature to check for repeatability and consistency of the results. Figure 4.1, Figure 4.2 and Figure 4.3 show the results of the BBR creep experiments performed on binders satisfying PG 58-34, PG 64-28 and PG 64-22 grades respectively.

Only in the first trial (Trial-1) of the BBR tests, creep experiments were performed on each of the 12 beam samples at three different temperatures T_{ref}, T_{ref} + 6°C and T_{ref} + 12°C, this was not done for the Trial-2 and Trial-3 experiments. The same beam was used for testing at multiple temperatures during the Trial-1 experiments and different beams were used for Trial-2 and Trial-3 experiments. If a particular trial did not meet the ASTM 6648-08 (2016) criterion for repeatability the entire test data corresponding to the Trial-1 were removed from further analysis.

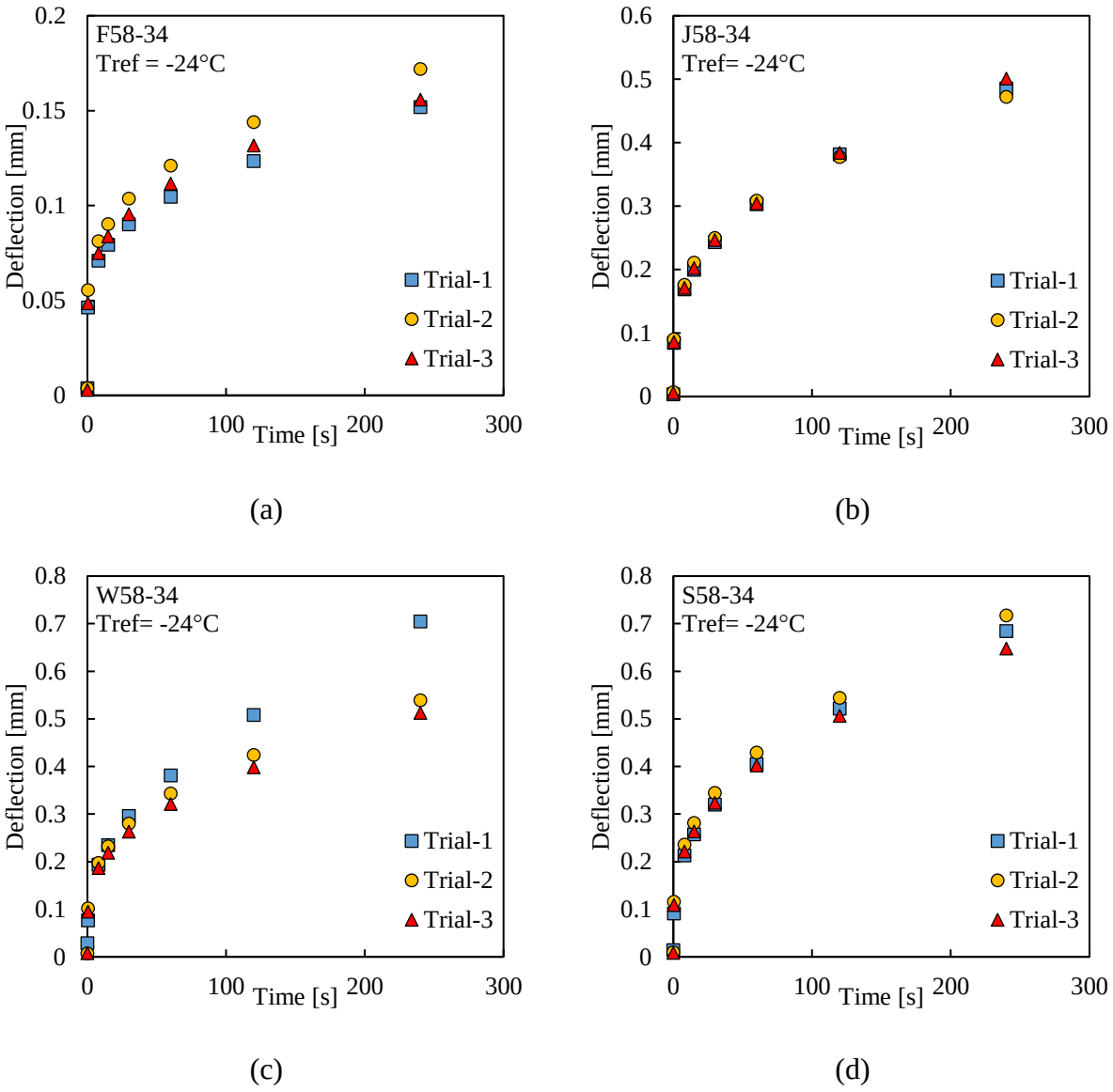

Figure 4.1 BBR deflection vs. time for three replicate samples for PG 58-34 grade binders at a reference temperature of -24°C: (a) Flint Hills, (b) Jebro, (c) WSA, (d) Suncor.

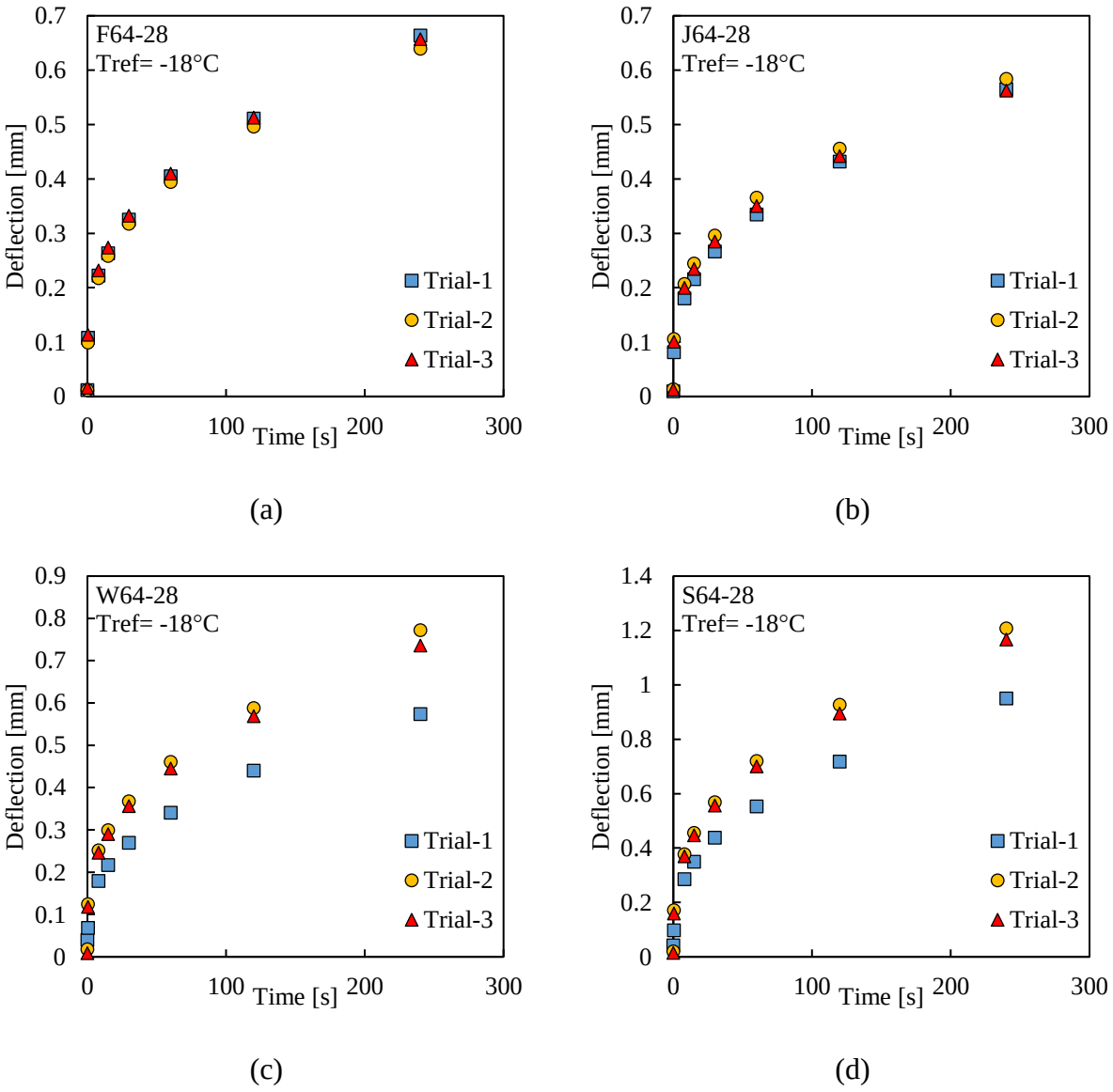

Figure 4.2 BBR deflection vs. time for three replicate samples for PG 64-28 grade binders at a reference temperature of -18°C: (a) Flint Hills, (b) Jebro, (c) WSA, (d) Suncor.

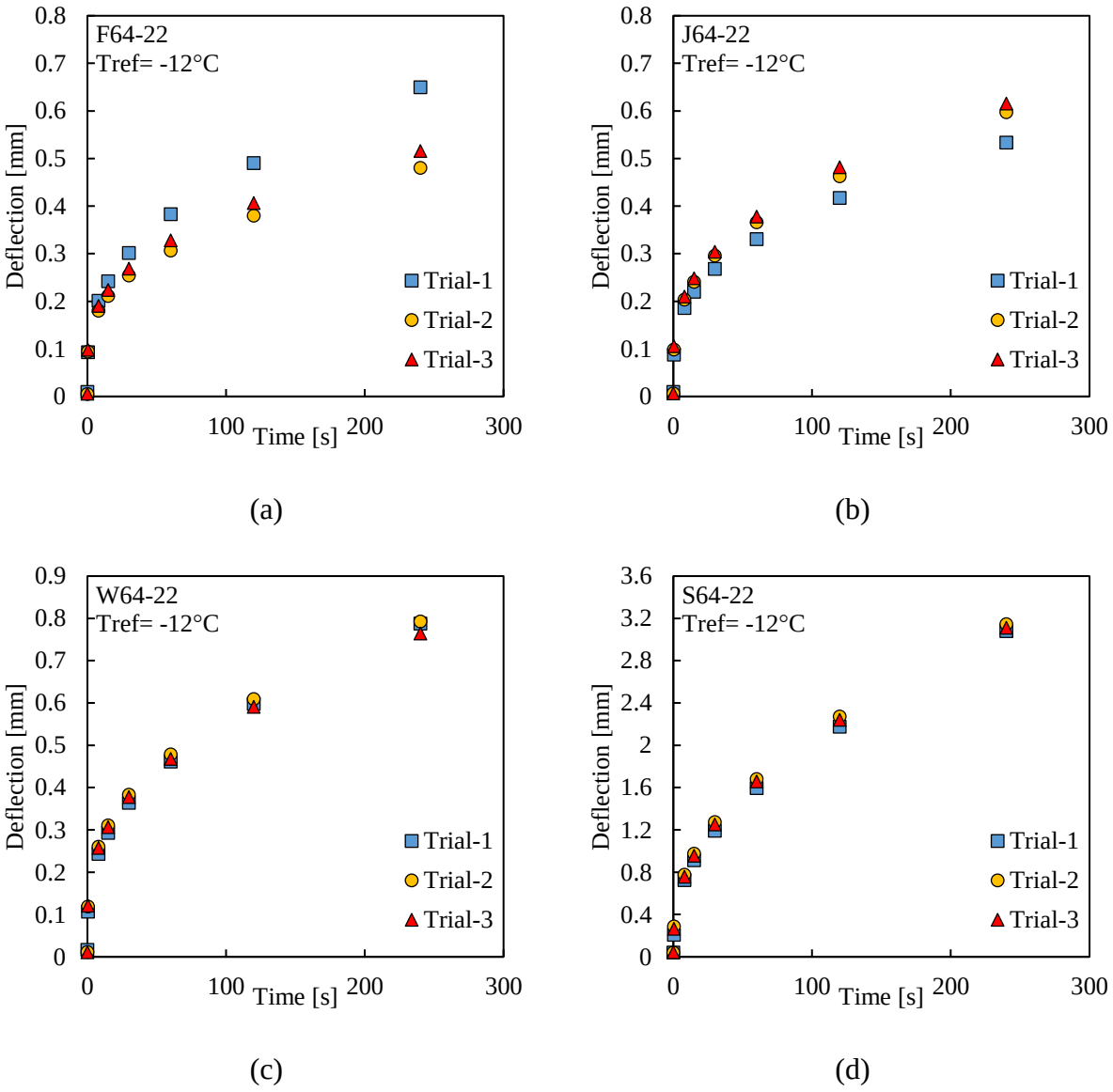

Figure 4.3 BBR deflection vs. time for three replicate samples for PG 64-22 grade binders at a reference temperature of -12°C: (a) Flint Hills, (b) Jebro, (c) WSA, (d) Suncor.

Table 4.1 shows the stiffness $S(t=60s)$ and slope $m(t=60s)$ calculated for the binder set used in the current investigation. Data corresponding to the temperature T_{ref} for a given binder is the average of two or three replicates as discussed in the previous section whereas, data corresponding T_{ref}+6°C and T_{ref}+12°C are the result of a single attempt (Trial-1). Table 4.1 represents the comprehensive data set for BBR creep test results for the 12 binders used in the current investigation. Table 4.1 shows that, for some binder samples corresponding T_{ref}+6°C and T_{ref}+12°C results are, missing; this is due to the fact that the corresponding Trial-1 data did not meet the ASTM repeatability criterion and was removed from the analysis. The data set shown in

Table 4.1 is used for further analysis such as correlations and deflection predictions based on DSR experiments utilizing different methodologies described in the following sections.

Table 4.1 BBR Test Average Stiffness and Slope Values at t=60s for All Binders Tested at T_{ref}

Sample	Temperature [°C]	BBR (Averaged Data)	
		***S*(*t*=60s) [MPa]**	***m*(*t*=60s)**
F58-34	-24	690.05	0.23
	-18	455.02	0.29
	-12	186.82	0.37
F64-28	-18	198.29	0.33
	-12	105.00	0.40
	-6	48.18	0.52
F64-22	-12	253.79	0.30
W58-34	-24	241.20	0.31
W64-28	-18	176.07	0.34
W64-22	-12	170.55	0.34
	-6	89.70	0.39
	0	41.39	0.52
J58-34	-24	262.13	0.31
	-18	128.49	0.39
	-12	55.48	0.45
J64-28	-18	228.93	0.33
	-12	112.75	0.40
	-6	47.93	0.49
J64-22	-12	218.56	0.33
S58-34	-24	194.26	0.34
	-18	99.98	0.41
	-12	42.44	0.50
S64-28	-18	112.15	0.35
S64-22	-12	48.29	0.43
	-18	153.35	0.34

4.2 DSR Test Results

Linear viscoelastic properties of each of the 12 binders described in Table 3.3 were obtained in the form of master curves for storage modulus ($G'(\omega)$), loss modulus ($G''(\omega)$) and phase angle (δ) at the reference temperature (T_{ref}). The testing scheme for performing the frequency sweep tests is described in Chapter 3. The master curves are representative of the material-specific, temperature and time-dependent mechanical properties of each binder. Intermediate temperature

(65 °C to 0 °C) testing of the binder using DSR are usually performed using the 8-mm parallel plate geometry and tests using this geometry are usually avoided at temperatures below 0 °C due to increased stress levels and necessary compliance correction. Recently Sui et al. (*12*, *13*) explored the use of 4-mm parallel plate as a suitable geometry for binder rheological characterization at very low temperatures. With necessary compliance correction (*12*, *13*, *43*) either of the two geometries can be used for binder rheological tests at freezing temperatures in the range of 0 °C to -40 °C. Hence in the current investigation 8-mm parallel plate was employed for most of the DSR frequency sweep experiments, additionally; 4-mm plate experiments were also conducted on a set of randomly selected samples. The 4-mm experiments were performed for determining the plate/geometry independence between the 4-mm and 8-mm plates when obtaining the rheological properties below 0 °C.

Figure 4.4 shows the complex modulus (|*G**|) values for three different PG grade binders. Figure 4.4(a), (b) and (c) show the master of the |*G**| values for PG 58-34, PG 64-28 and PG 64-22 binders tested in the current study. The master curves were obtained at the corresponding low temperature PG grade +10 °C.

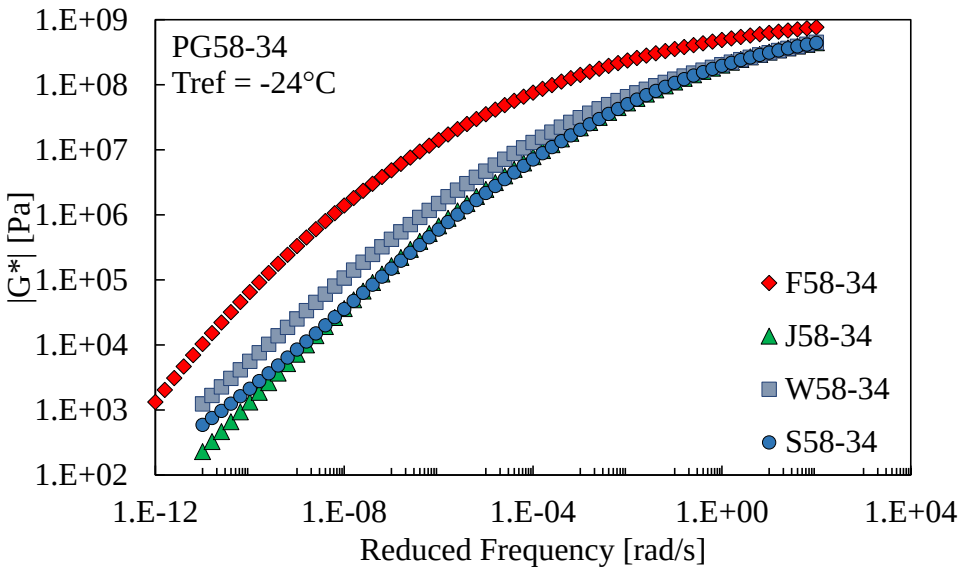

(a)

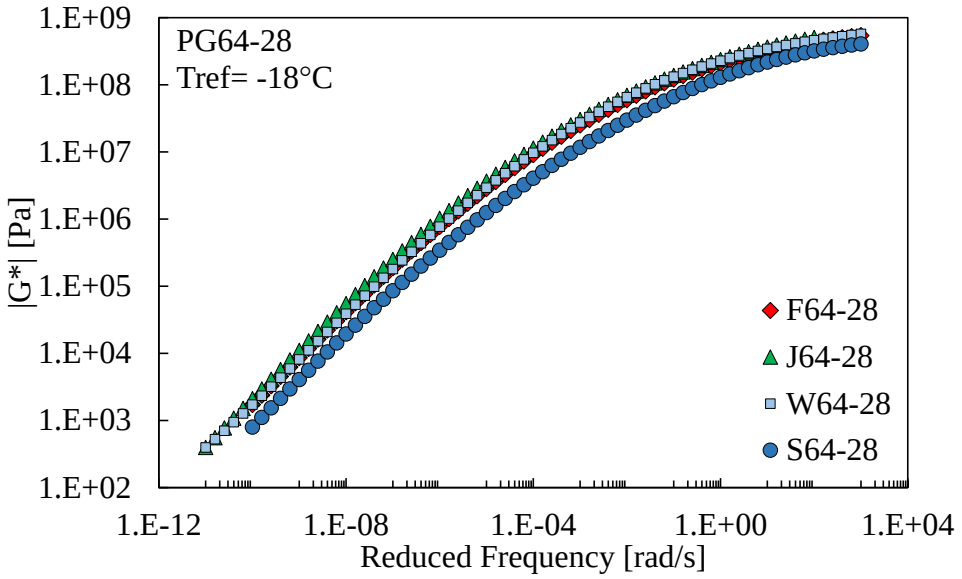

(b)

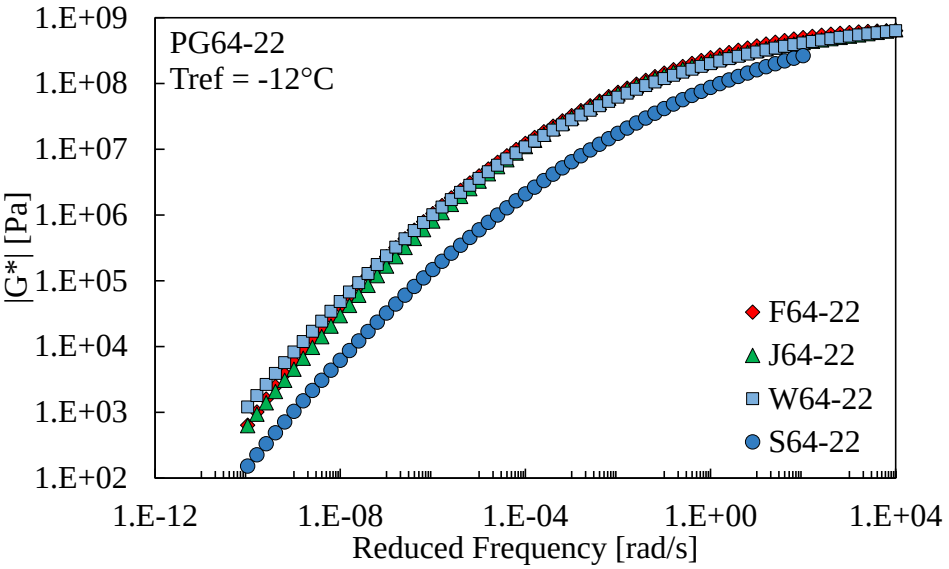

(c)

Figure 4.4 Master curve of |*G**| values using trial-1 data: (a) PG 58-34, (b) PG 64-28, and (c) PG 64-22 grade binders performed by 8-mm parallel plate.

Additionally, to investigate the influence of plate geometry on the rheological properties of the binder at low temperatures, frequency sweep tests were performed on several samples using the 4-mm parallel plate geometry. Four binders shown in Table 3.4 were randomly selected from the sample group and tested using the 4-mm parallel plate. The testing scheme and methodology adopted for the 4-mm geometry were similar to those used for 8-mm geometry such that similar testing conditions were maintained. Also, necessary compliance correction was

automatically performed using the rSpace software of Malvern Kinexus DSR that was used to control the experiments. Figure 4.5 shows the |*G**| master curves of the four binders. As shown, the master curve results were quite similar and does not depend on the type of geometry used for performing the oscillatory tests at temperatures below 0 °C. With necessary steps such as compliance correction and normal force control for variable gap are considered with precise sample trimming conditions when performing the experiments, a good match between the 8-mm and 4-mm parallel plate geometry were achieved.

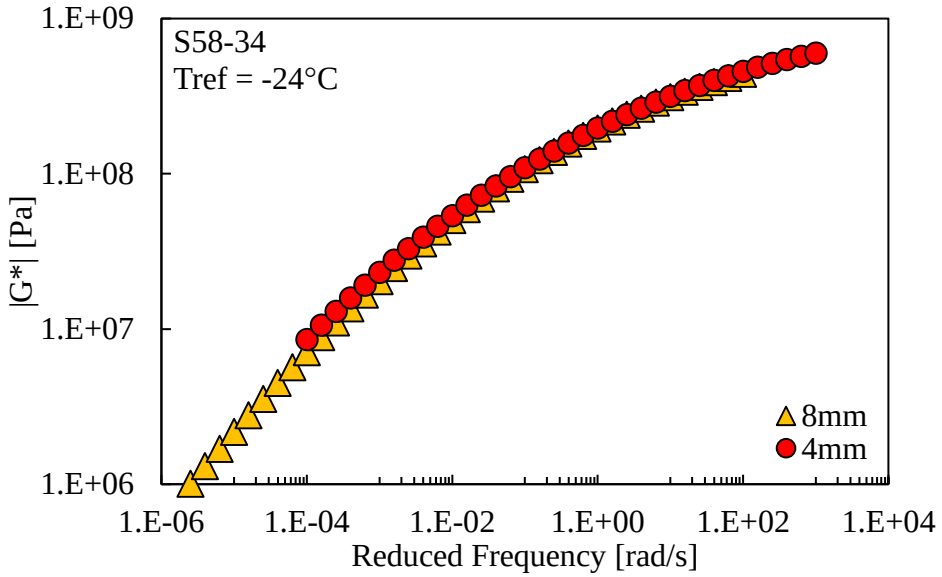

(a)

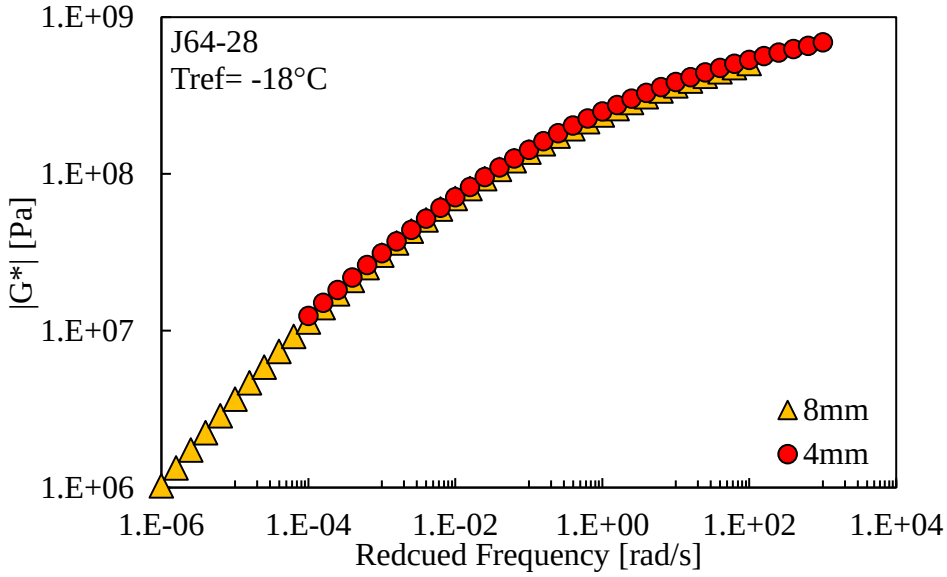

(b)

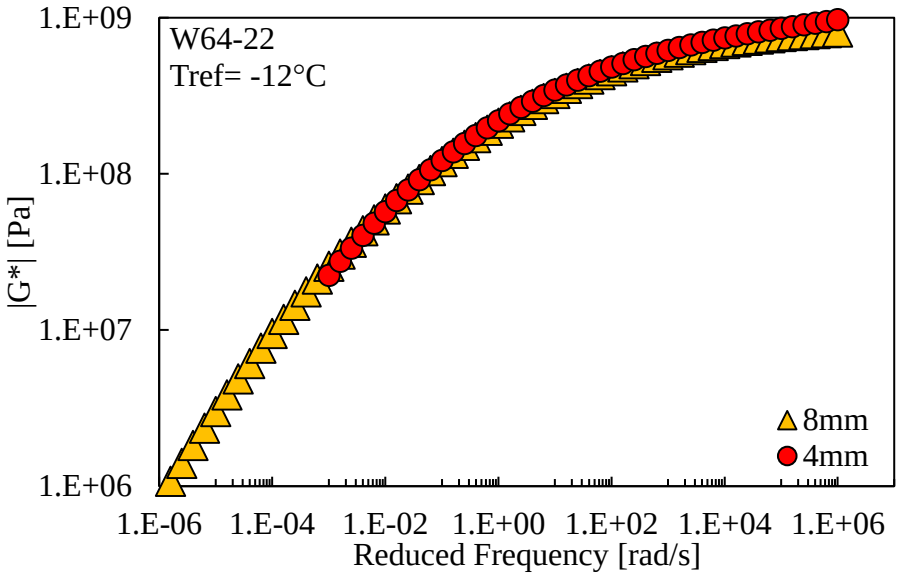

(c)

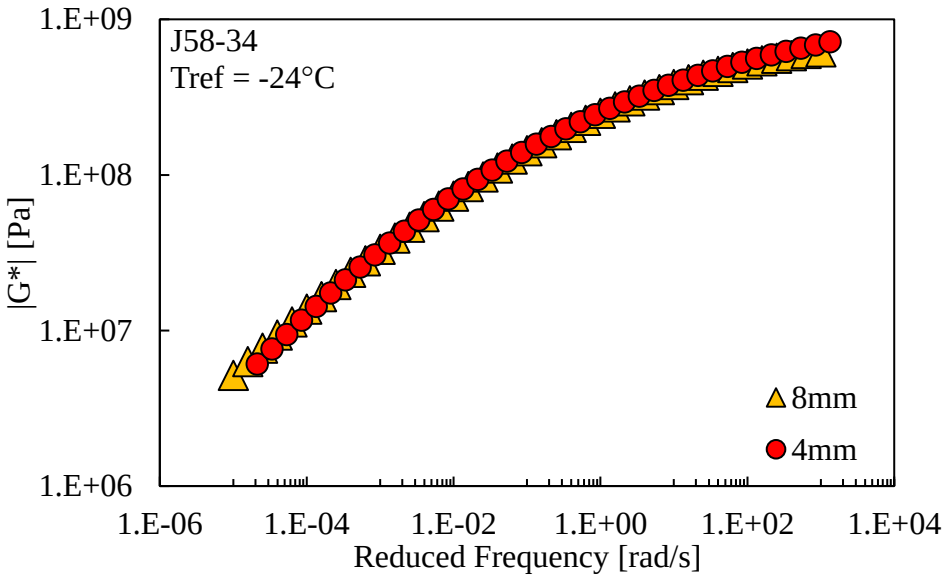

(d)

Figure 4.5 Master curve of |*G**| using 4-mm and 8-mm parallel plate geometry: (a) S58-34, (b) J64-28, (c) W64-22, (d) J58-34.

4.3 WRI Methodology

Sui et al. (*12, 13*) and Farrar et al. (*14*) investigated the use of DSR to measure and characterize the low temperature rheological properties of binder using the 4-mm parallel plate rheology. They found a strong correlation between BBR stiffness (slope of stiffness) data and relaxation

modulus (slope of relaxation modulus) of binders measured at time t = 60s and temperature PG+10 °C. Based on these correlations Farrar et al. (*14*) developed an alternative low temperature grading criterion at Western Research Institute (WRI). The fundamental idea in the WRI methodology is to obtain cutoff parameters similar to the BBR stiffness ($S(t)$) and slope ($m_{BBR}(t)$) criterion through measurements made using the 4-mm parallel plate DSR. In this method an equivalent cutoff relaxation modulus ($G(t)$) and slope (m_{DSR}) parameters were established through linear correlation between data obtained using the DSR and BBR. The shear relaxation modulus $G(t)$ as a function of time was obtained by converting the master curve of the frequency dependent storage modulus ($G'(\omega)$) test data at the reference temperature (T_{ref}) of PG+10 °C. The interconversion from frequency domain to time domain was then conducted using the approximated equation given by Christensen (*51*) as shown in Equation 4.1.

$$G(t) \approx G'(\omega)\big|_{\omega=2/\pi t} \tag{4.1}$$

The procedure adopted for implementing the WRI methodology to the binders selected in the current investigation is described next. Based on the low temperature PG grade of the selected binder, frequency sweep data of four temperatures close to the low PG grade were selected for WRI analysis. As an example, if a binder that satisfies PG 58-34 was selected, frequency sweep data at temperatures of -24 °C, -18 °C, -12 °C and -6 °C were selected and a master of the $G'(\omega)$ was constructed. Figure 4.6 (a) and (b) show the storage modulus ($G'(\omega)$) at different temperatures and the master curve of $G'(\omega)$ respectively at a reference temperature of T_{ref} = -24°C for sample S58-34. Figure 4.6 (c) shows the interconverted frequency domain $G'(\omega)$ to shear relaxation modulus $G(t)$. A second order polynomial is fitted to the log($G(t)$) vs. log(t) data and the corresponding value of $G(t$=60s) and slope ($m_{DSR}(t$=60s)) is calculated using the fitted equation. Similarly, $G(t$=60s) and $m_{DSR}(t$=60s) is obtained for all the binders investigated in the current study for correlating or comparing with the corresponding BBR stiffness $S(t$=60s) and $m_{BBR}(t$=60s).

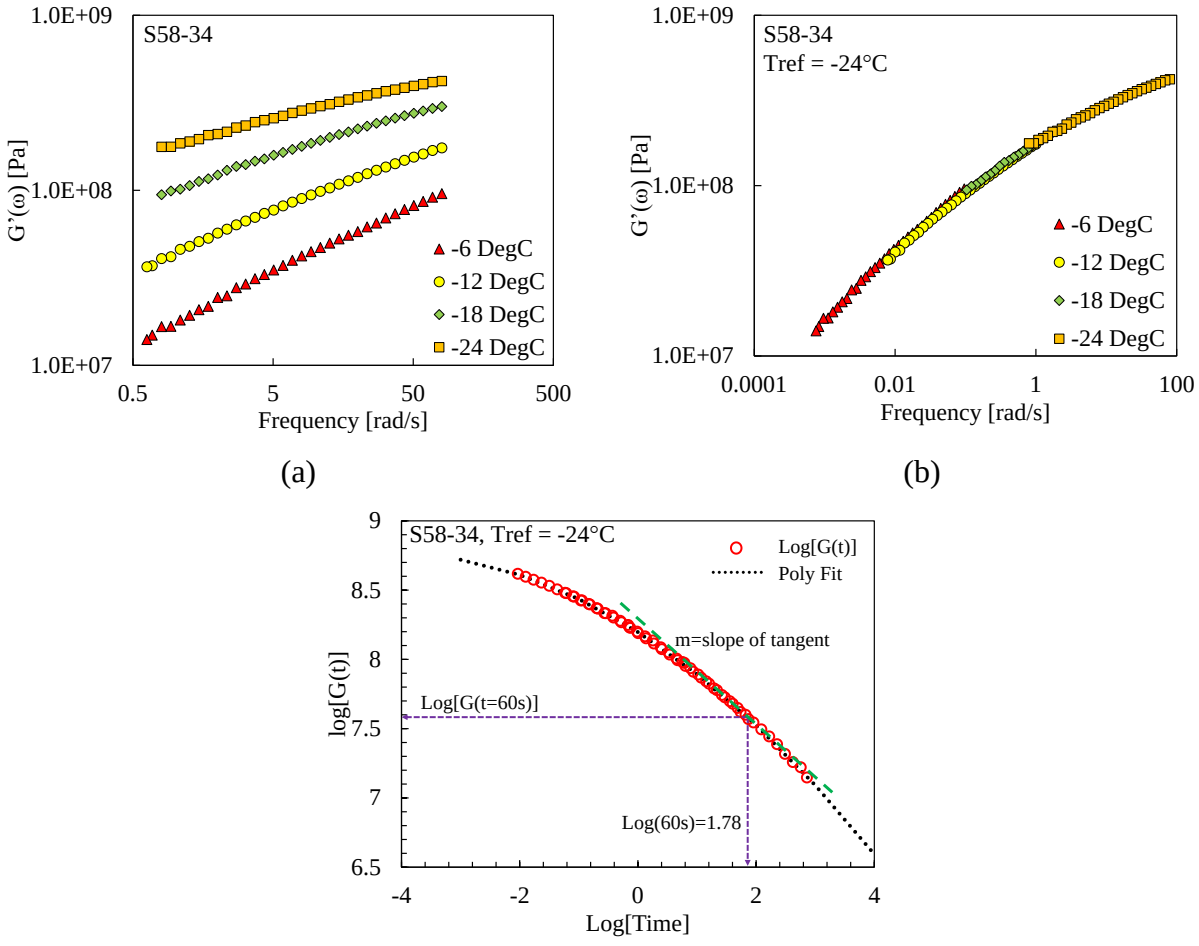

Figure 4.6 Example of WRI methodology for sample S58-34: (a) storage modulus at different temperatures, (b) master curve of the storage modulus at T_{ref}= -24°C, (c) method for obtaining $G(t=60s)$ and $m(t=60s)$.

In order to fully utilize this methodology, it is necessary to have a good data base that covers a range of binder grade specifications such that, the relaxation modulus and slope criterion can be calibrated according to the binders used in a specific region or State, in this study, the state of Nebraska.

Figure 4.7 shows the result of applying the WRI methodology to the binders selected in this study. Generally, good linear correlations were observed when comparing the DSR relaxation modulus $G(t=60s)$ and slope m_{DSR} results with the corresponding creep stiffness $S(t=60s)$ values and slope $m_{BBR}(t=60s)$ of the BBR tests. For the binder data base selected in the current study the low temperature grading criterion was established to limiting the shear modulus $G(t=60s) < 85.35$ MPa and absolute slope of the $G(t)$ vs. t curve at $t=60s$ to be $m_{DSR}(t=60s) >$

0.287, as shown in Table 4.2. It can be observed that the limiting criterion are different for the relaxation modulus as compared to the WRI estimation. This demonstrates that the methodology is strongly dependent on the binder data base selected and it is necessary to calibrate the method more often to meet the state DOT's current practice. Nonetheless, the slope limiting value obtained from the Nebraska binder data set is close to the value proposed by WRI as shown in Table 4.2. The binders often tend to fail at the slope criterion earlier than the relaxation modulus criterion, either of the limiting values can be considered. Alternatively, for more strict grading criterion, the calibrated values from the Nebraska binder dataset can be used and updated-recalibrated as new binders are introduced into the dataset.

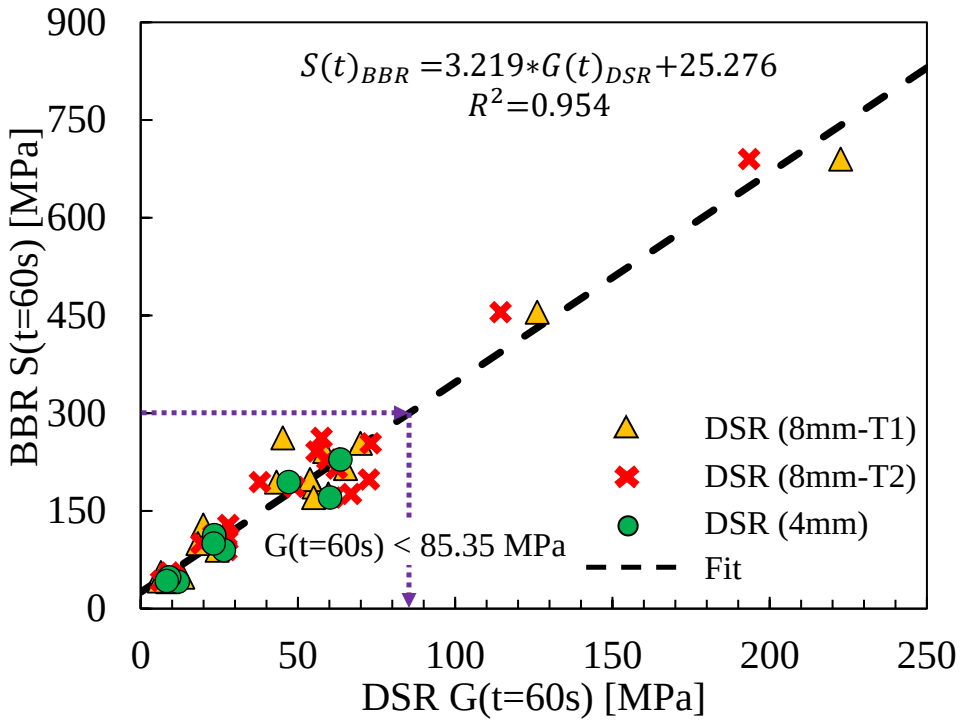

(a)

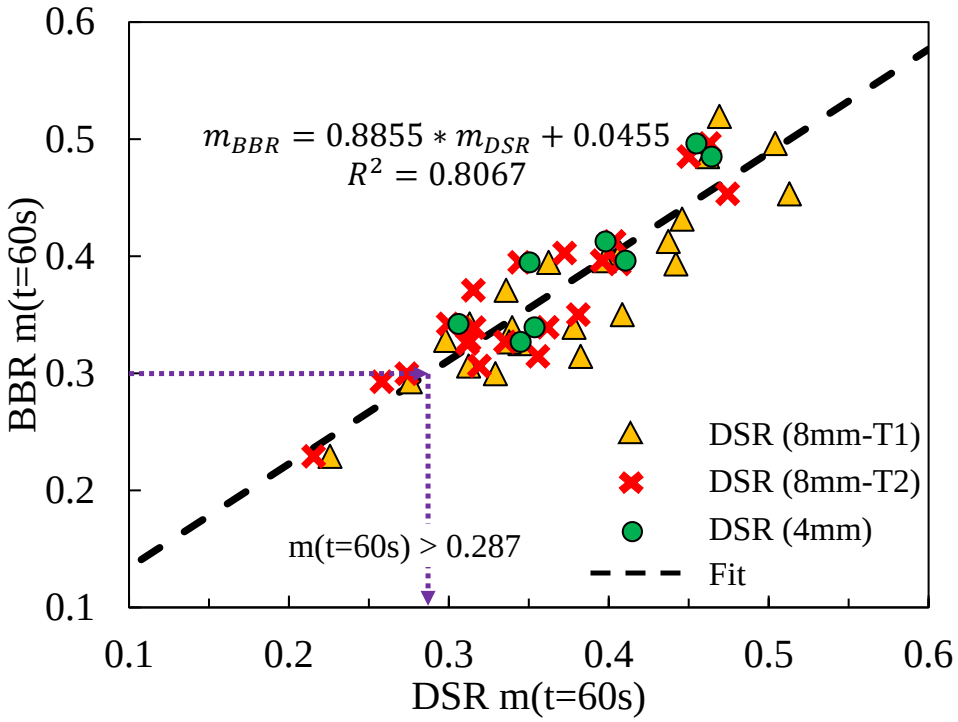

(b)

Figure 4.7 (a) Correlation between $S_{BBR}(t=60s)$ and $G_{DSR}(t=60s)$, (b) correlation between $m_{BBR}(t=60s)$ and $m_{DSR}(t=60s)$.

Table 4.2 Comparison of WRI Criterion Using Nebraska Binders

Binder Data Set	***G*(*t*) at *t*=60s**	***m*(*t*) at *t*=60s**
WRI	143 [MPa]	0.28
Nebraska	85.35 [MPa]	0.287

4.4 NCHRP Methodology

During the NCHRP program (*2*) for characterizing binder properties, researchers had investigated the idea of interconverting dynamic shear test data to flexural creep data. They presented a method for converting the complex shear modulus data at intermediate temperatures to creep stiffness at freezing temperatures where the BBR tests were performed. A similar

approach termed as the NCHRP methodology was thus investigated here for the binder data set used in this study. The advantage of this methodology lies in the fact that DSR tests can be performed at relatively much higher temperatures compared to the BBR test temperature and then shifted to the corresponding low temperature using simple shift factors.

The range of the intermediate temperature for performing the DSR frequency sweep tests depends on the low temperature grade of the binder selected. Relevant frequency sweep tests performed using DSR within this temperature range can be converted to the corresponding stiffness $S(t)$ data using Equation 4.2.

$$S(t) \approx \frac{3G^*(\omega)}{[1 + 0.2\sin(2\delta)]}, t \rightarrow {}^{1}/_{\omega} \tag{4.2}$$

where $S(t)$ [Pa] is the creep stiffness as a function of time t [s], $G^*(\omega)$ [Pa] is the complex modulus as a function of frequency ω [rad/s] and δ is the phase angle at the corresponding frequency.

Since BBR tests are performed at relatively low temperatures close to PG+10°C and measurements are made at time t=60s, the stiffness data obtained from DSR tests need to be shifted to the BBR test temperature. The shift factor applied to the DSR stiffness data is based on the Arrhenius equation as shown in Equation 4.3.

$$\log\left(\frac{t_{ref}}{t}\right) = \frac{E_a}{2.303\,R}\left[\frac{1}{T_{ref} + 273} - \frac{1}{T + 273}\right] \tag{4.3}$$

where t_{ref} and T_{ref} are the reference time [s] and temperature [°C] (related to BBR test conditions) respectively, t and T are the testing time [s] and temperature [°C] (related to the intermediate DSR tests), respectively, and E_a is activation energy and R is ideal gas constant 8.31 [J/°K-mol]. The value of $\frac{t_{ref}}{t}$ is termed as the shift factor (a_T^{time}) in the time domain.

Usually the activation energy parameter is dependent on the binder rheological response as a function of temperature that is unique to a given binder, whereas in the NCHRP methodology, this parameter was fixed at 250,000 [J/mol]. Table 4.3 shows the target frequency needed for the DSR frequency sweep at different intermediate temperatures to represent the

loading time of t=60s for the corresponding reference temperature (T_{ref}) where the BBR data are obtained. Table 4.3 was obtained using the Equation 4.3.

Table 4.3 Target Frequency for DSR Test to Represent t=60 s Loading Time of the BBR Test

BBR-Test (T_{ref}) Temperature [ºC]	**Target DSR ω[rad/s]**			
	-12ºC	**-6ºC**	**0ºC**	**10ºC**
-24	4.30	57.36	682.18	33,474.67
-18	0.25	3.34	39.76	1,951.25
-12	0.02	0.22	2.64	129.62

As an example of the NCHRP methodology, binder satisfying PG 58-34 was selected; in this case F58-34. The appropriate temperature (T= -12°C) for the dynamic frequency sweep test to be performed on the binder using DSR is selected from Table 4.3. Based on the table, the DSR frequency sweep tests could be performed at either T= -12°C or T= -6°C since the corresponding frequencies are well within the ranges (0.1 rad/s to 100 rad/s) that are normally applied to binders. Figure 4.8 (a) shows the frequency sweep performed on the binder in the range of 0.6 to 80 rad/s. Figure 4.8 (b) shows the $G^*(\omega)$ data converted to creep stiffness $S(t)$-DSR using the Equation 4.2, the $S(t)$-DSR data is shifted to T_{ref} = -24°C at which the BBR experiments are performed using the shift factor obtained using Equation 4.3. It can be seen in Figure 4.8 (c) that the NCHRP method gives a reasonable estimate of the stiffness prediction. Figures 4.9 to 4.11 further demonstrate the predictability of the NCHRP methodology.

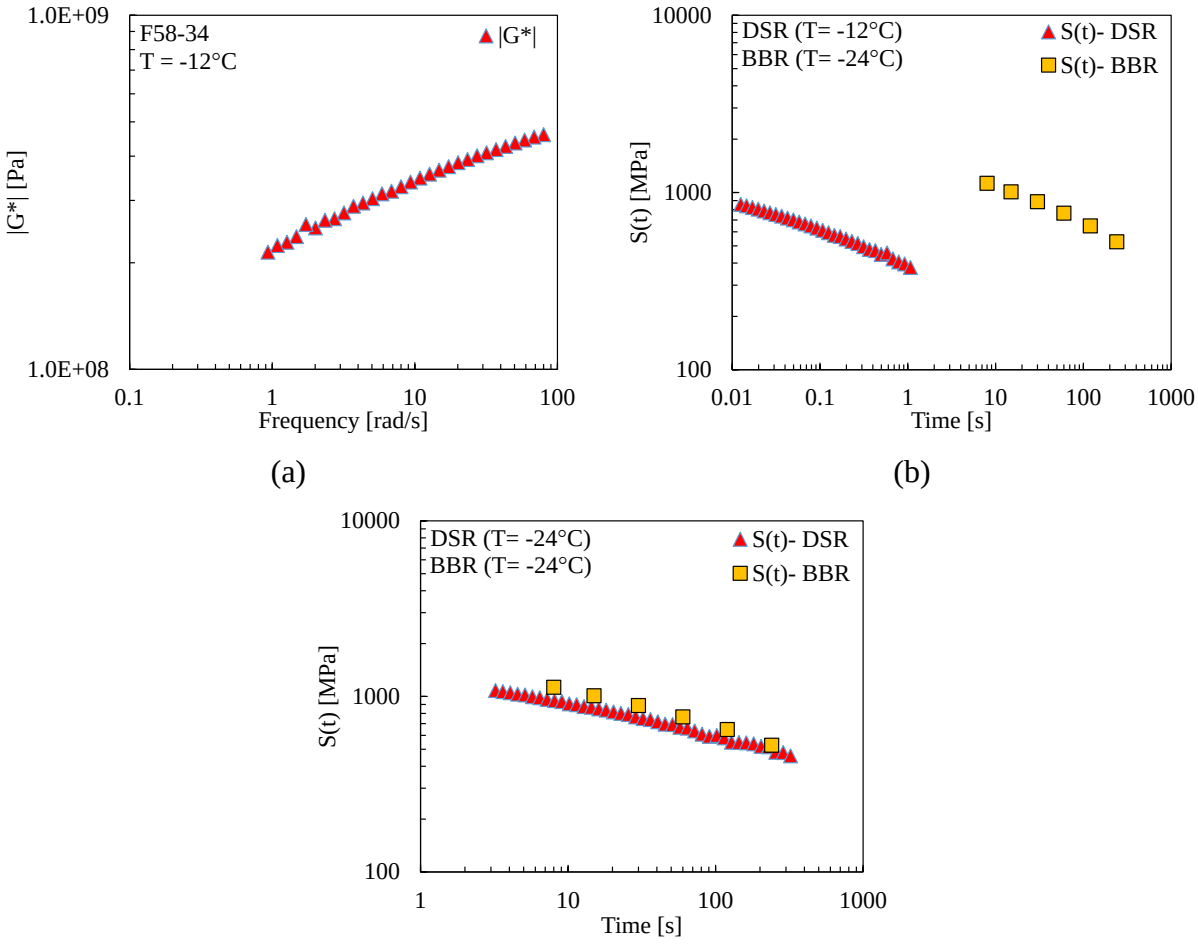

Figure 4.8 Application of NCHRP methodology on F58-34 binder: (a) frequency sweep performed at T= -12°C, (b) converted $S(t)$ using Equation 4.2 at T= -12°C, (c) shifted $S(t)$-DSR and the experimental $S(t)$-BBR.

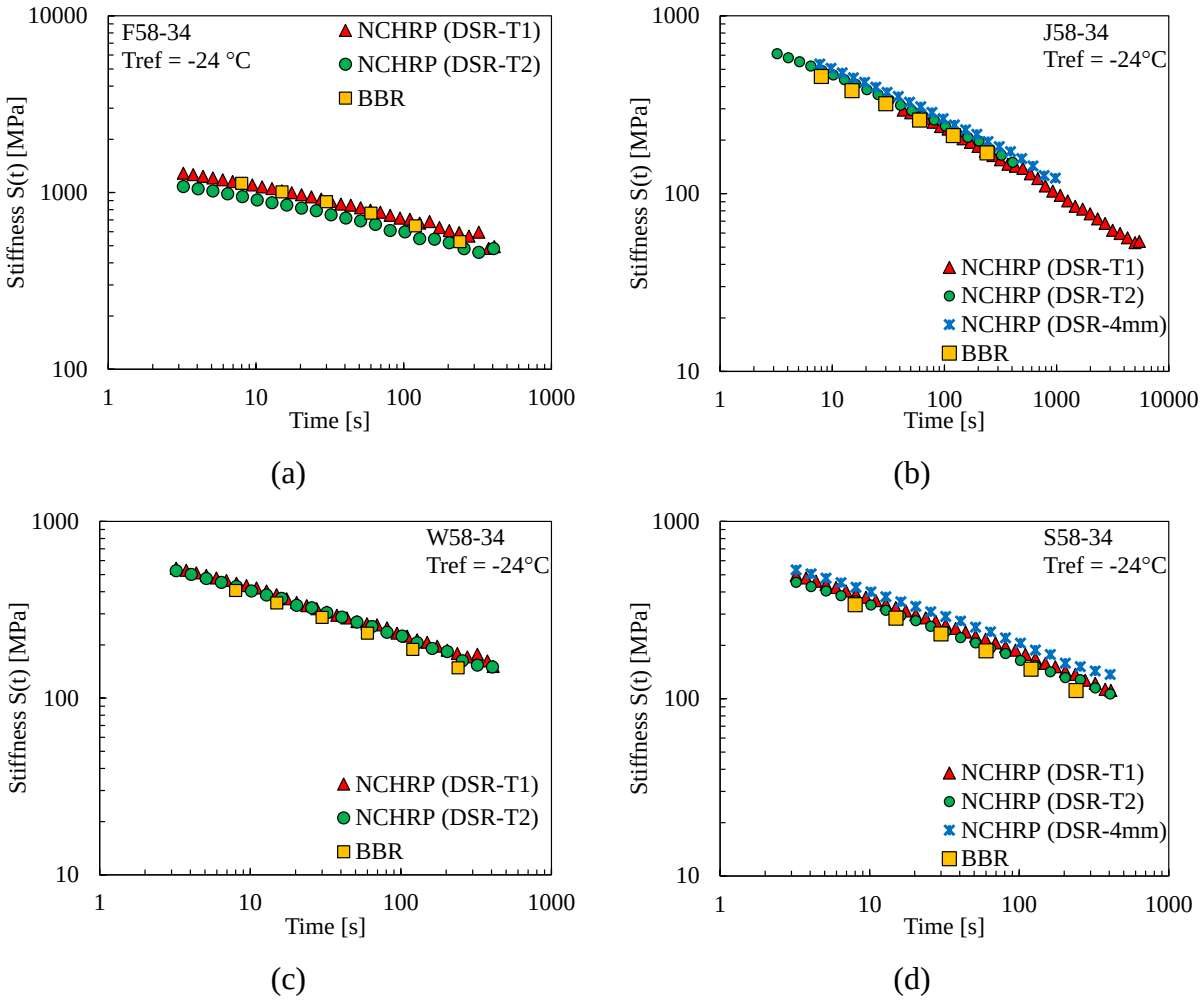

Figure 4.9 NCHRP methodology applied to all PG 58-34 grade binders: (a) F58-34, (b) J58-34, (c) W58-34, (d) S58-34.

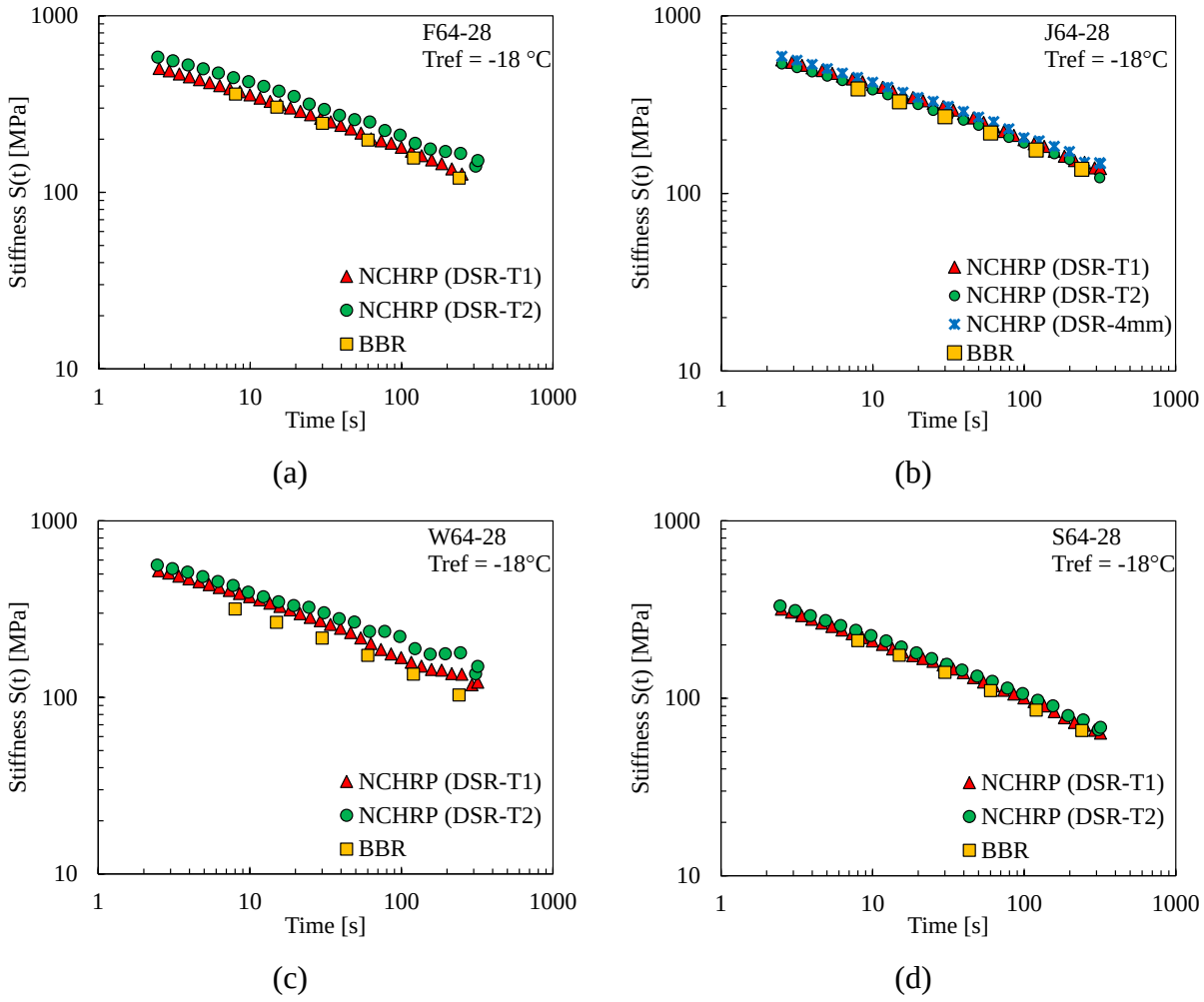

Figure 4.10 NCHRP methodology applied to all PG 64-28 grade binders: (a) F64-28, (b) J64-28, (c) W64-28, (d) S64-28.

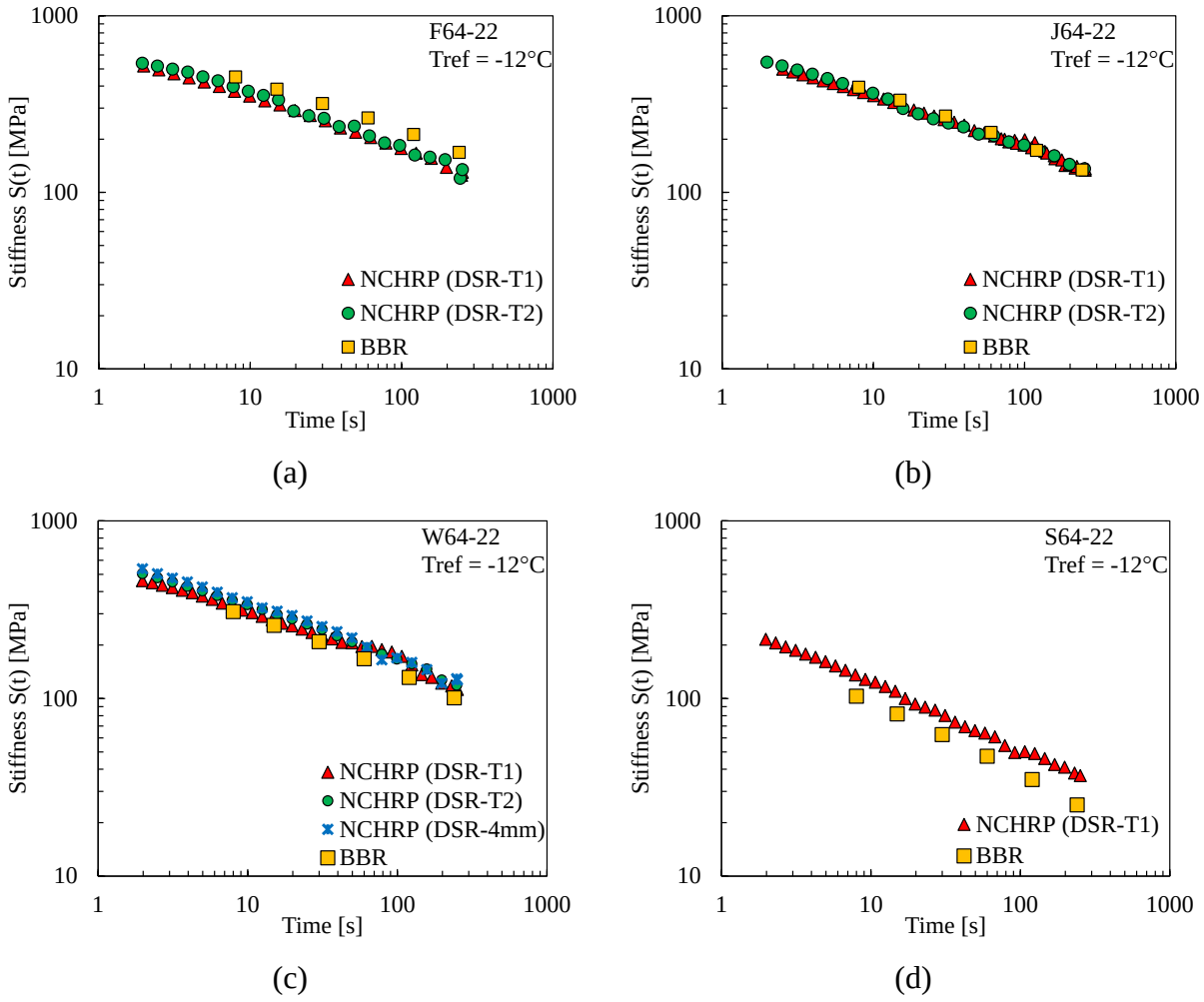

Figure 4.11 NCHRP methodology applied to all PG 64-22 grade binders: (a) F64-22, (b) J64-22, (c) W64-22, (d) S64-22.

Similarly, the NCHRP method described in Figure 4.8 was applied to all the binders represented in Table 3.3 and Table 3.4. Figure 4.12 shows the linear correlation for the stiffness $S(t=60s)$ and $m(t=60s)$ obtained using the NCHRP method and experimental BBR data. In Figure 4.12 (a) it can be observed that stiffness predictions using the NCHRP method are reasonably accurate as shown by the closeness of the linear fit to the line of equality. In Figure 4.12 (b) it can be observed that slope predictions using the NCHRP method deviate from the line of equality and mostly underpredict the BBR experimental values. This can be attributed to the use of single activation energy (E_a) used for shifting the DSR-$S(t)$ data for different binders, usually this parameter is specific and unique to a given binder.

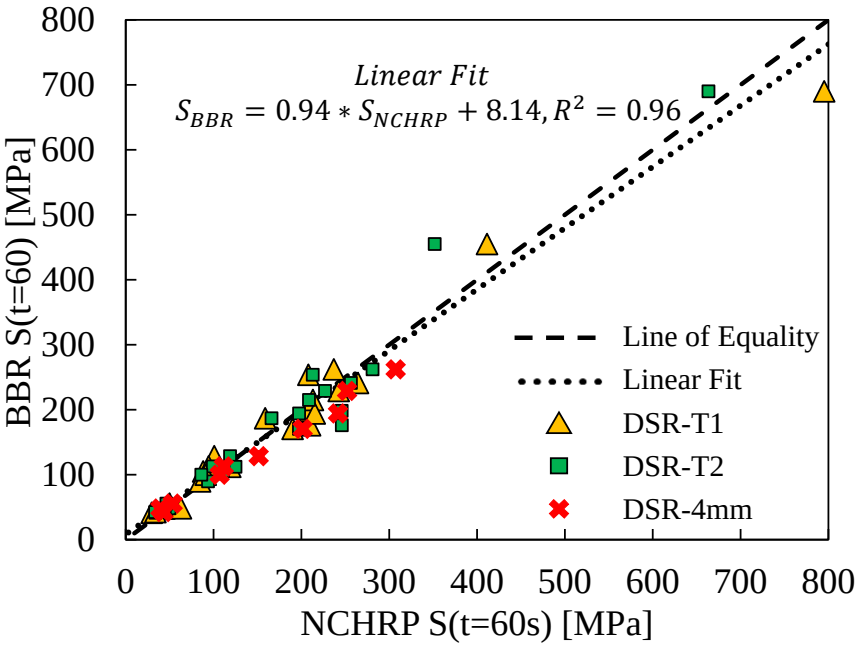

(a)

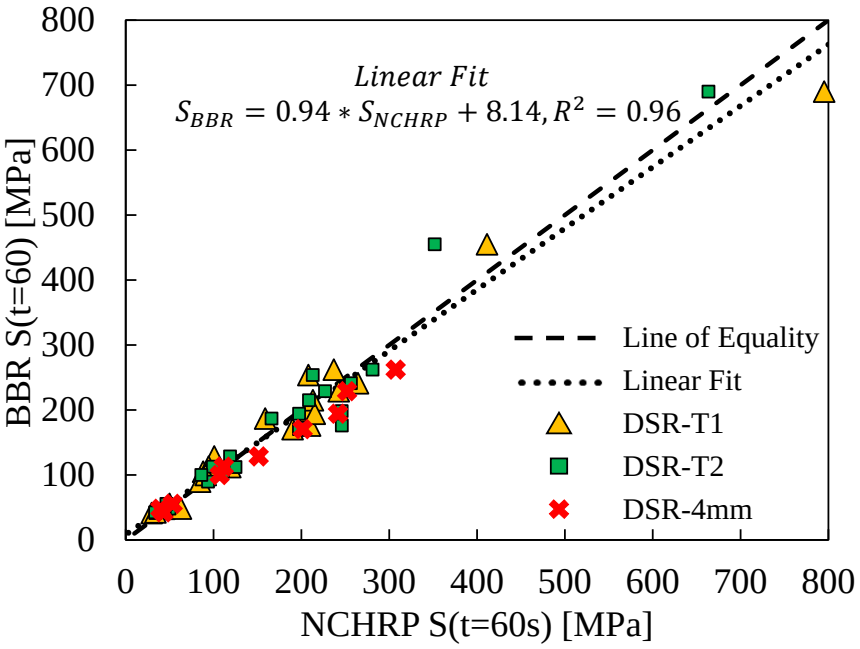

(b)

Figure 4.12 Correlation between (a) stiffness *S*(*t*=60s), (b) slope *m*(*t*=60s) obtained using NCHRP method and experimental BBR data.

4.5 UNL's Mechanistic Approach

Linear models such as the generalized Maxwell and Voigt models were used in the current study to represent the binder viscoelastic material properties. Use of such models allows one to describe the time dependent response of asphaltic materials under various temperature and loading conditions. In order to obtain the relaxation modulus, $G(t)$ the linear viscoelastic models were used to describe the response of the binder. Amongst all the models the generalized Maxwell and Kelvin-Voigt models have been widely utilized for modeling asphaltic materials due to the ease of representing these models in the form of Prony series which are quite flexible in terms of usage during any numerical efforts.

Equations 4.4 and 4.5 show the Prony series representation of the relaxation modulus $G(t)$ and the creep compliance $J(t)$ where $G_0, G_i, J_g, J_i, \rho_i, \tau_i$ and η_i are model parameters that need to be estimated for each binder.

$$G(t) = G_0 + \sum_{i=1}^{m} G_i e^{\left(-t/\rho_i\right)} \tag{4.4}$$

$$J(t) = J_g + \frac{t}{\eta_i} + \sum_{i=1}^{n} J_i \left(1 - e^{\left(-t/\tau_i\right)}\right) \tag{4.5}$$

The frequency domain representation of the Prony series is shown in Equations 4.6 and 4.7. Using the equations one can fit the experimental data to obtain the material-dependent viscoelastic model parameters. Schapery et al. (*52*) discussed in detail the different methods of obtaining these parameters and also interconverting from one form to another in the time domain. Similar approach was utilized in this study to obtain the material specific properties for all 12 binders.

$$G'(\omega) = G_0 + \sum_{i=1}^{m} \frac{G_i \omega^2 \rho_i^2}{(\omega^2 \rho_i^2 + 1)} \tag{4.6}$$

$$G''(\omega) = \sum_{i=1}^{m} \frac{G_i \omega \rho_i}{(\omega^2 \rho_i^2 + 1)} \tag{4.7}$$

As an example, Figure 4.13 shows the Prony fit for the *G'* and *G''* that were used to obtain the material parameters of the binder J64-28 using the method described by Schapery et al. (*52*). Similarly, the binder specific material parameters were obtained for each binder.

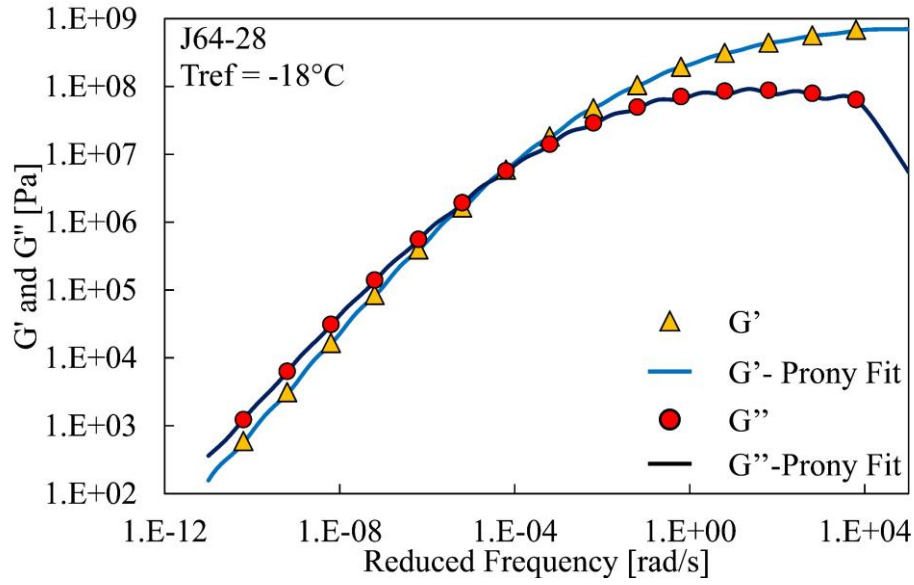

(a)

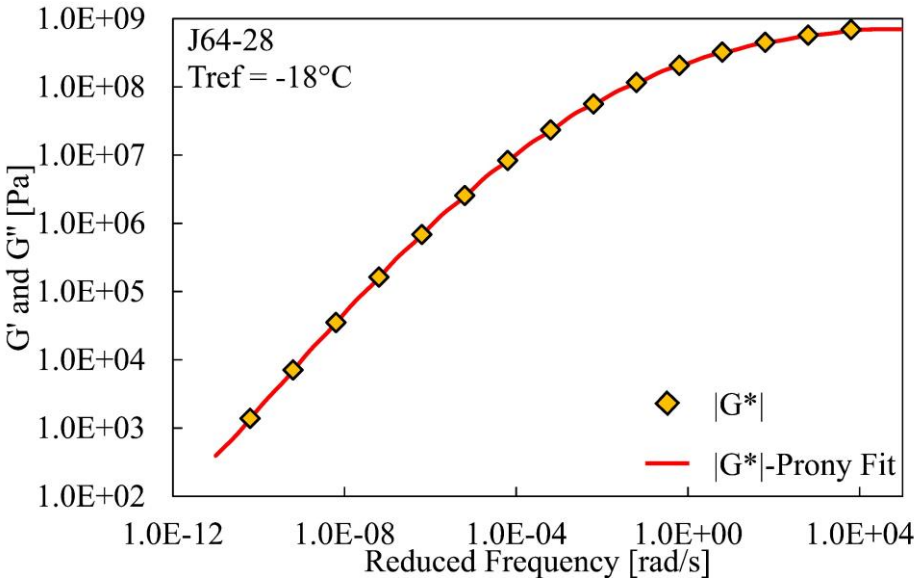

(b)

Figure 4.13 Prony fit to the experimental data: (a) $G'(\omega)$ and $G''(\omega)$ data, (b) $|G^*|$ data for J64-28 at T_{ref} = -18°C.

Based on the elastic-viscoelastic correspondence principle one can use the general beam theory for the deflection of an elastic beam to obtain solutions for similar viscoelastic problems. The UNL's mechanistic approach is based on the elastic-viscoelastic correspondence principle. Equation 4.8 shows the time-dependent beam deflection, Δ(t) that was obtained using the elastic-viscoelastic correspondence principle for a three-point bending beam testing on a viscoelastic material. Here, $J(t)$ is the time-dependent creep compliance at the temperature corresponding to $T=T_{ref}$ that one needs to obtain from the DSR testing, $P(t)$ is the time-dependent load applied at the center of the beam, v is the Poisson's ratio of the viscoelastic material which can be assumed to be 0.5 for binder and I is the second moment of inertia of the beam sample. The goal is to predict the experimental BBR beam deflections from the DSR test results using the solution described in Equation 4.8.

$$\Delta(t) = \frac{J(t)}{2(1+v)} \frac{L^3}{48I} P(t) \tag{4.8}$$

4.5.1 Comparing BBR deflection results to DSR predictions

After obtaining the creep compliance function for each binder based on the method described in the previous section, one can predict the linear viscoelastic beam deflections subjected to mechanical loads similar to the BBR experiment using Equation 4.8. The stiffness $S_{DSR}(t=60s)$ and $m_{DSR}(t=60s)$ are obtained using the method described in ASTM 6648-08 (2016). An example of the predicted beam deflections for binder sample J58-34 at different test temperatures is shown in Figure 4.14 (b) (c) and (d). The corresponding $|G^*|$ master curves from the three trials is shown in Figure 4.14 (a). It can be observed that Equation 4.8 somewhat overpredicts the deflection results from the DSR tests when compared to the experimental BBR results. Another observation is that even though a good repeatability was observed from the DSR frequency sweep experiments (Figure 4.14(a)), there were nontrivial differences in the deflection predictions. This difference can be attributed to multiple reasons including: (1) small change in the logarithmic scale representation of modulus values can result in a relatively large difference in linear-scale prediction of beam deflection, (2) the relaxation modulus Prony series terms identified through the fitting process of the $|G^*|$ master curves can be different for different trials, hence the subsequent interconversion process can result in different creep compliance

parameters, and (3) different cooling media and equilibration time used for the two tests (DSR and BBR) can result in unequal physical hardening effects.

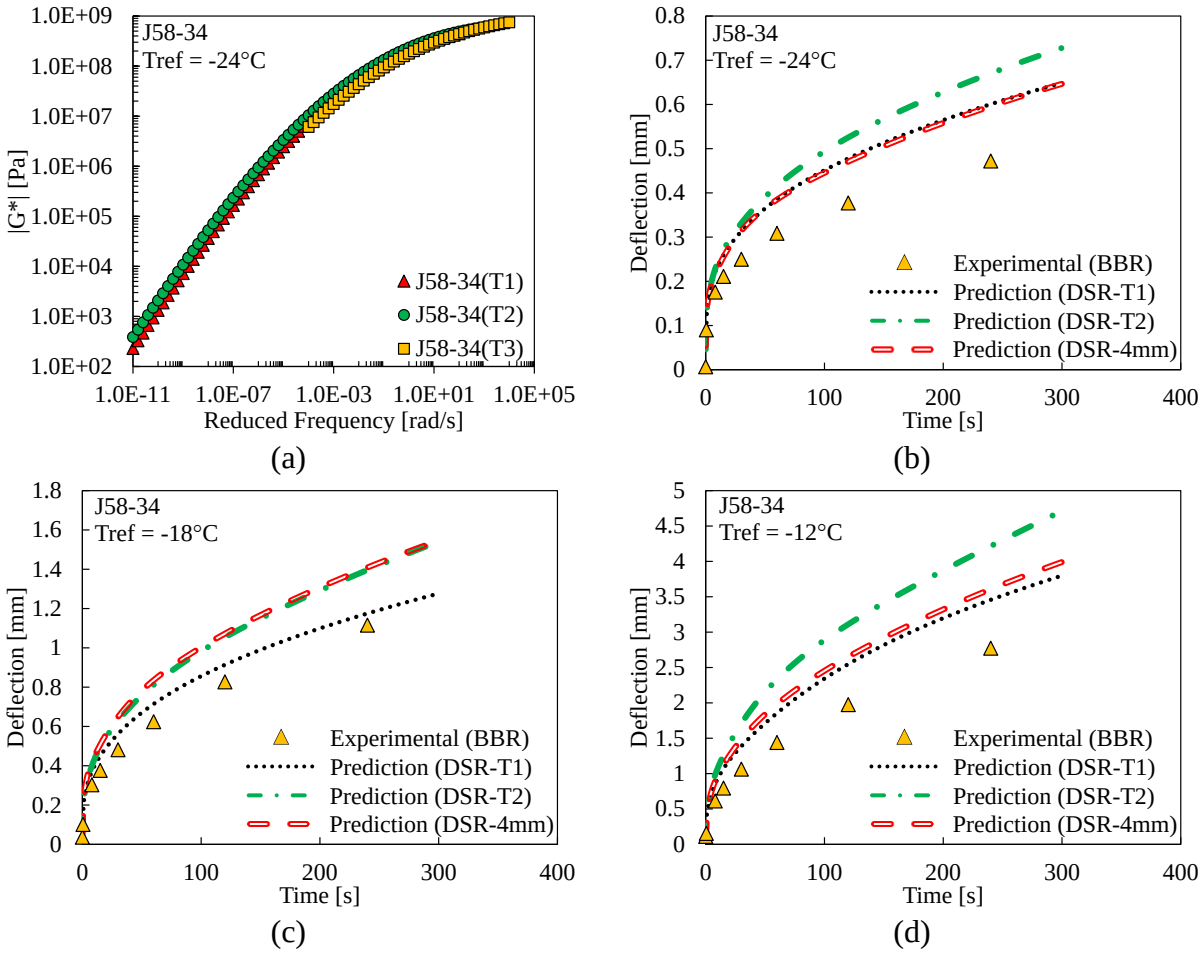

Figure 4.14 DSR data of J58-34 binder where (a) |G*| Master curves for different trials. DSR deflection results at (b) T_{ref} = -24°C (c) T_{ref} = -18°C and (d) T_{ref} = -12°C.

Equation 4.8 was utilized to predict the BBR results for all the binders. Figure 4.15 (a) and (b) compare the DSR prediction with BBR results for creep stiffness ($S(t)$) and slope m-value, respectively. It can be observed that the UNL mechanistic method (using the linear viscoelastic correspondence principle) generally underpredicts the stiffness and slope values for most of binders.

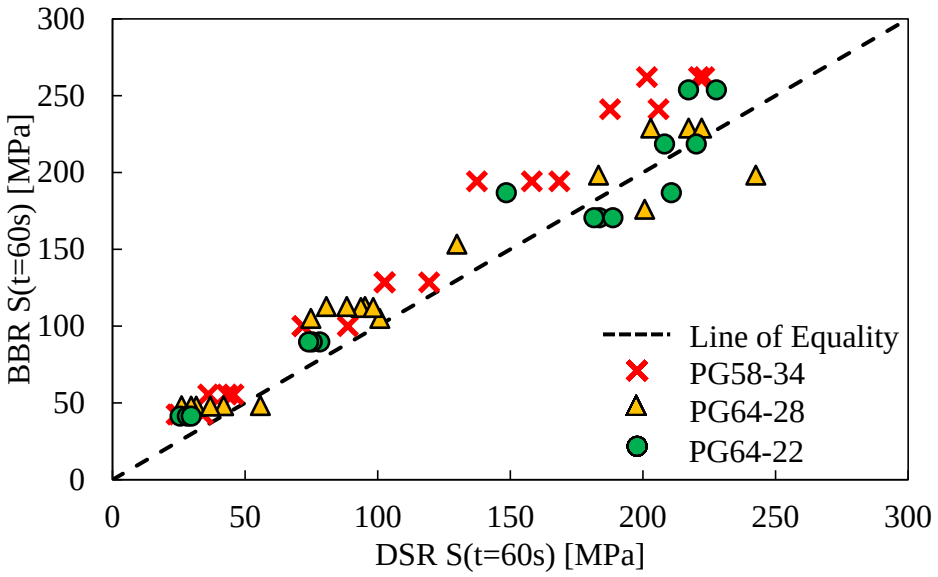

(a)

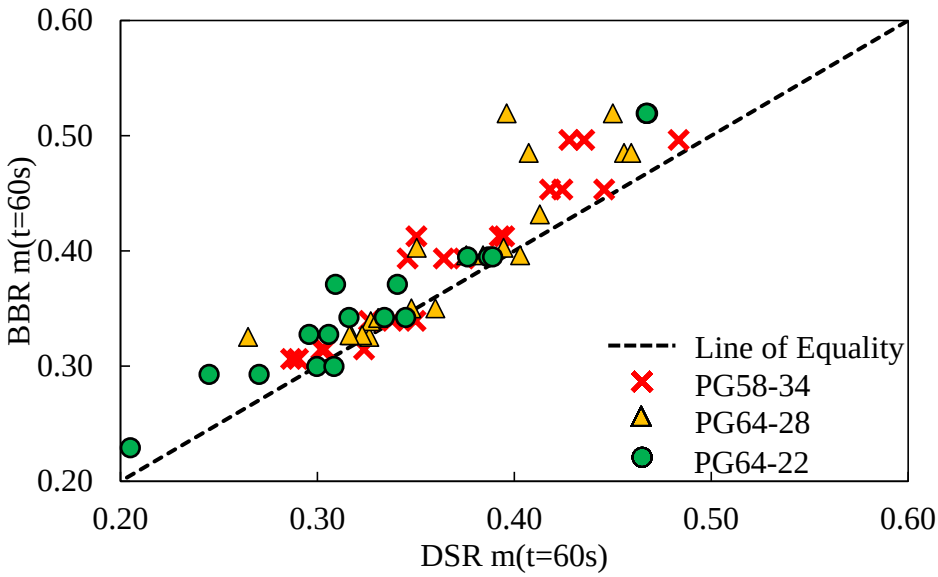

(b)

Figure 4.15 (a) Comparison of the DSR predicted $S(t=60s)$ with the BBR $S(t=60s)$, (b) comparison of the DSR predicted $m(t=60s)$ with the BBR $m(t=60s)$ for PG 58-34, PG 64-28 and PG 64-22 binders.

From Figure 4.15, it was observed that a horizontal shift in the creep compliance function $J(t)$ using a single shift factor a_β is necessary to more accurately predict the BBR results. This factor was used to account for the difference in physical hardening effects due to the different conditioning time and cooling media. To account for these changes, Equation 4.8 was modified to the equation described below:

$$\Delta(t) = \frac{J\left(t/a_\beta\right)}{2(1+v)}\frac{L^3}{48I}P(t) \tag{4.9}$$

Figure 4.16 (d) (e) and (f) shows the predictions made using the modified Equation (4.9) for binder sample J58-34 at different reference temperatures, where the shift factor a_β was calibrated such that accurate predictions to the BBR data were obtained. The shift factor a_β was assumed to be dependent only on the binder and temperature. Similarly, the shift factor a_β was calibrated for all the binders selected in this study as shown in Table 4.4.

From Figure 4.16, one can conclude that a single shift factor a_β in Equation (4.9) can account for dependence on the binder source, difference in testing conditions such as cooling media, physical hardening and temperature. In Table 4.4 it can be observed that the shift factor a_β is highly dependent on the binder source and reference temperature at which the BBR experiments were compared. This can be attributed to the different hardening rates in the vicinity of the glass transition temperature for different binders. Also, for a given binder grade there was a significant difference in shift factor a_β which indicates that the parameter is binder-specific and is an intrinsic material property that is temperature dependent. Although additional experiments are necessary to completely characterize the shift factor, due to the limited data set available in this study, a global average value of the shift factor $a_\beta = 1.736$ was used as shown in Table 4.5.

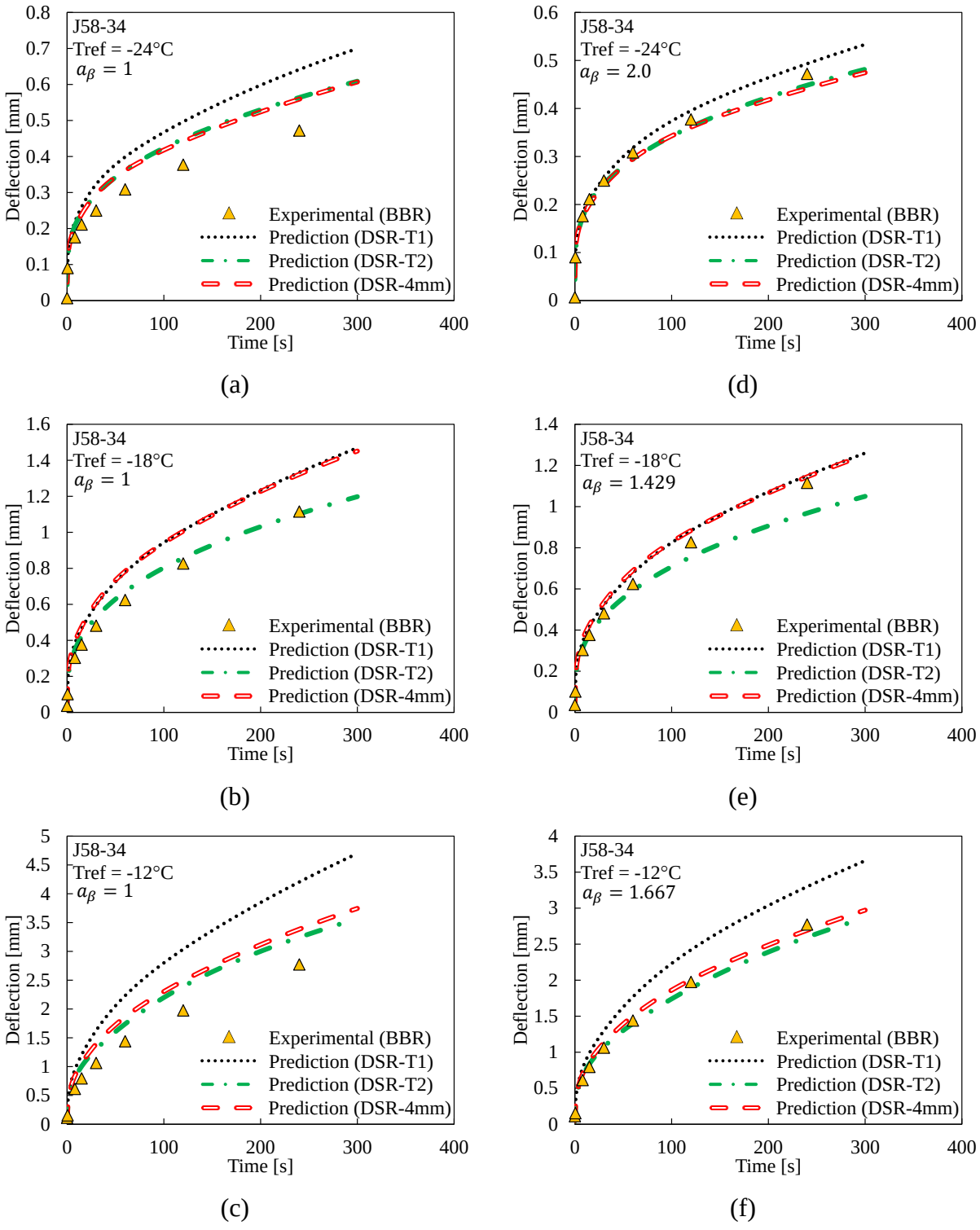

Figure 4.16 The influence of shift factor a_β for predicting BBR results for J58-34: (a) a_β =1, (d) a_β = 2.0 at T_{ref} = -24°C (b) a_β = 1, (e) a_β = 1.429 at T_{ref} = -18°C and (c) a_β = 1,(e) a_β = 1.667 at T_{ref} = -12°C.

Table 4.4 Shift Factor a_β Identified for Each Binder

Sample	Temperature	Factor
F58-34	-24	0.83
	-18	1.25
	-12	0.67
F64-28	-18	1.43
	-12	2.22
	-6	4.00
F64-22	-22	1.82
W58-34	-24	2.00
W64-28	-18	0.77
W64-22	-12	0.91
	-6	1.43
	0	2.50
J58-34	-24	2.00
	-18	1.43
	-12	1.67
J64-28	-18	1.43
	-12	2.00
	-6	2.86
J64-22	-12	1.25
S58-34	-24	2.00
	-18	2.00
	-12	1.67
S64-28	-18	1.82
S64-22	-12	0.67
	-18	1.72

Table 4.5 Average Shift Factor a_β of Each Different Group of Binder

PG 58-34	PG 64-28	PG 64-22	Global
1.814	1.893	1.462	1.736

Using the global shift factor a_β = 1.736 in Equation (4.9), the DSR predictions were compared to the BBR results, as shown in Figure 4.17, Figure 4.18 and Figure 4.19 for PG 58-34, PG 64-28, and PG 64-22, respectively.

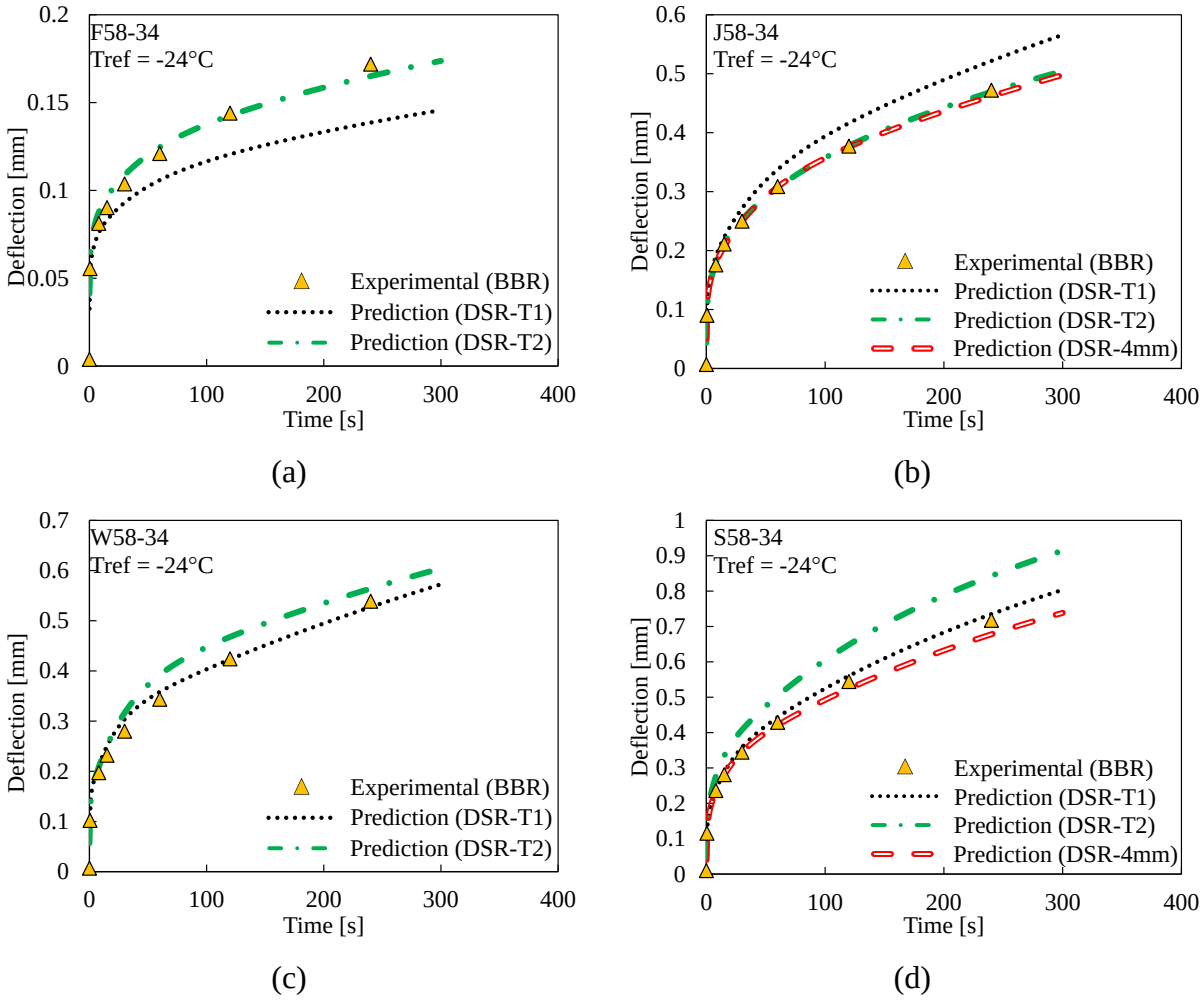

Figure 4.17 Comparison of the experimental BBR deflection results with DSR deflection prediction for PG 58-34 binders at reference temperature T_{ref}=-24°C and a_β =1.736 where (a) Flint Hills, (b) Jebro, (c) Western State Asphalt, (d) Suncor.

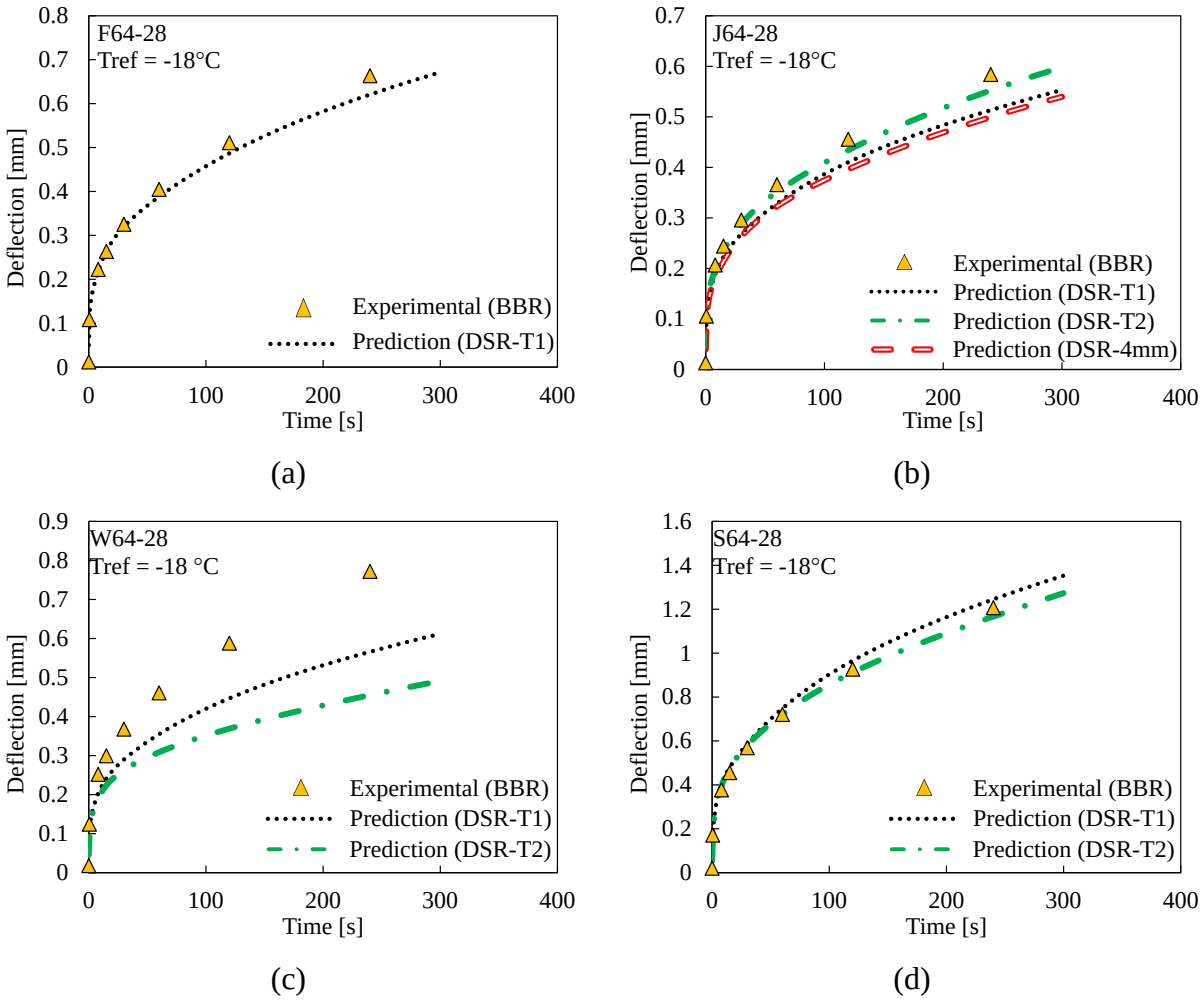

Figure 4.18 Comparison of the experimental BBR deflection results with DSR deflection prediction for PG 64-28 binders at reference temperature T_{ref}=-18°C and a_β =1.736 where (a) Flint Hills, (b) Jebro, (c) Western State Asphalt, (d) Suncor.

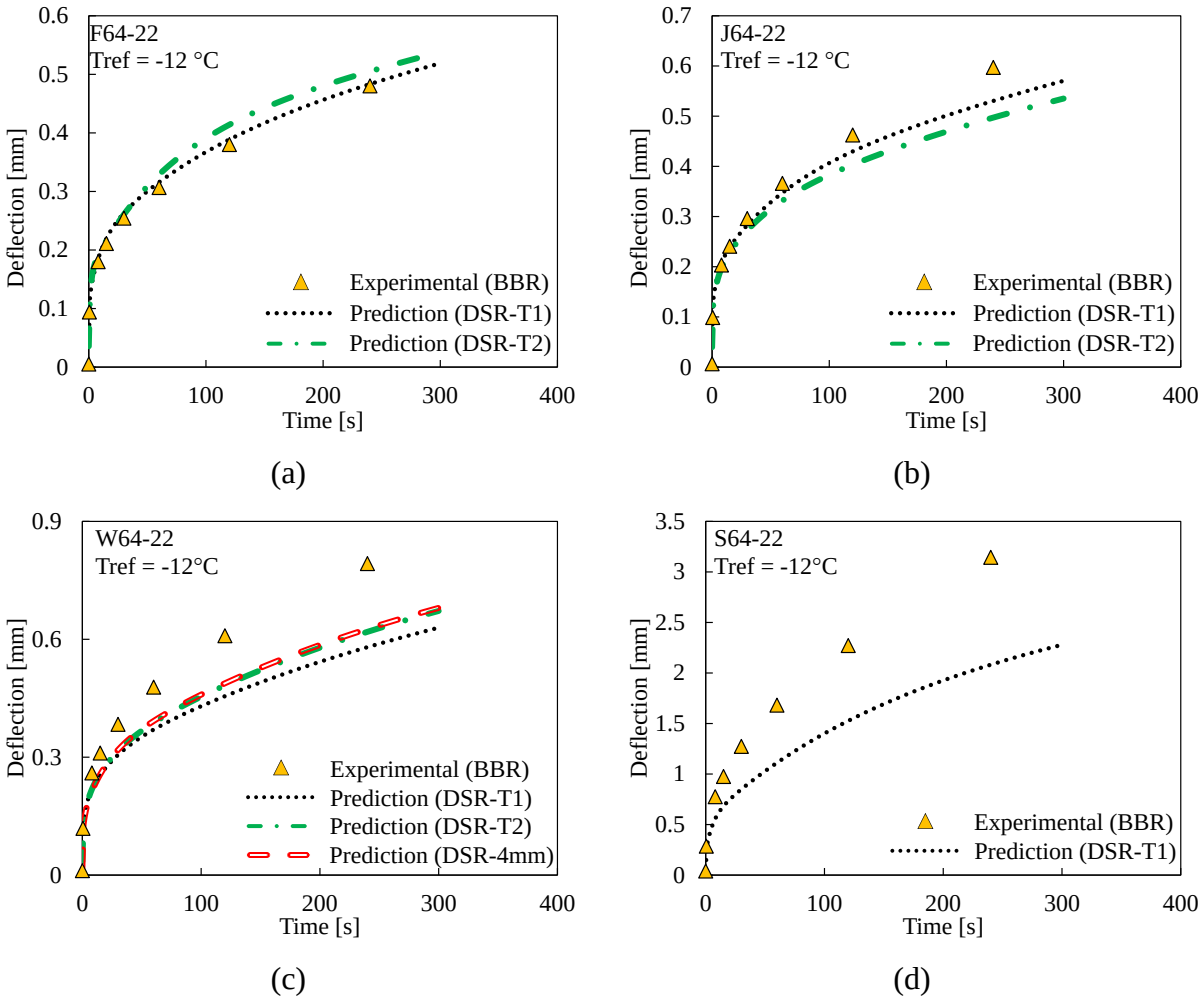

Figure 4.19 Comparison of the experimental BBR deflection results with DSR deflection prediction for PG 64-22 binders at reference temperature T_{ref}=-12°C and a_β = 1.736 where (a) Flint Hills, (b) Jebro, (c) Western State Asphalt, (d) Suncor.

4.5.2 Deflection predictions using DSR at different temperatures

One important advantage of testing with the DSR is that the testing scheme utilized for performing the frequency sweep experiment allows one to continuously asses the binder properties at any target temperature over a wide range of temperatures using the same set of data obtained without further conducting tests. This allows one to predict the BBR results at different temperatures using a single master curve.

Figure 4.20 and Figure 4.21 show the deflection predictions using the DSR results and a global average shift factor $a_\beta = 1.736$ at different target temperatures for samples J58-34, J64-28, W64-22 and S58-34. It can be observed that the global shift factor can satisfactorily predict BBR experimental results.

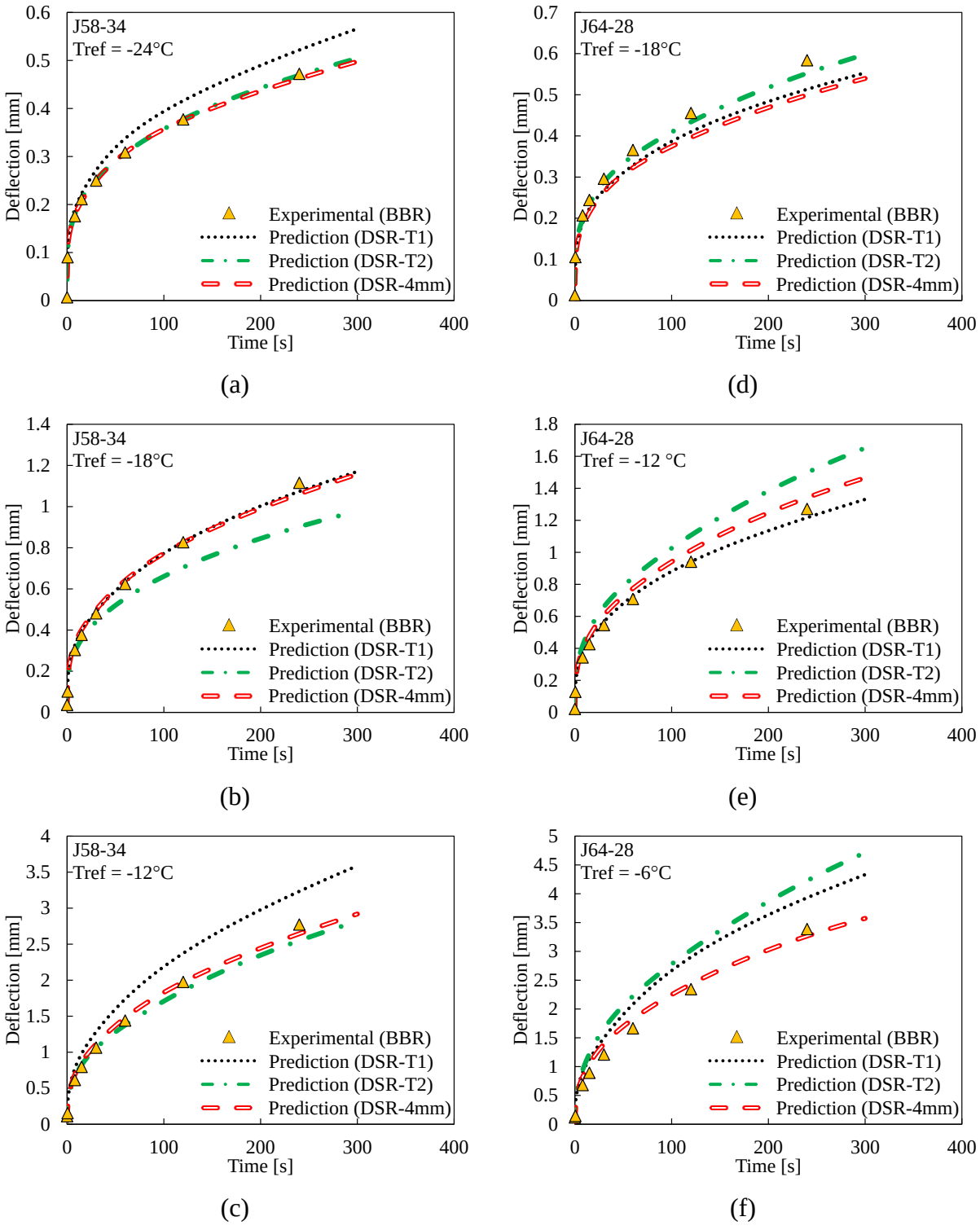

Figure 4.20 DSR beam deflection prediction at different temperatures with a_β = 1.736 for binders: J58-34 at (a) T_{ref} = -24°C (b) T_{ref} = -18°C (c) T_{ref} = -24°C and J64-28 (d) T_{ref} = -18°C (e) T_{ref} = -12°C (f) T_{ref} = -6°C.

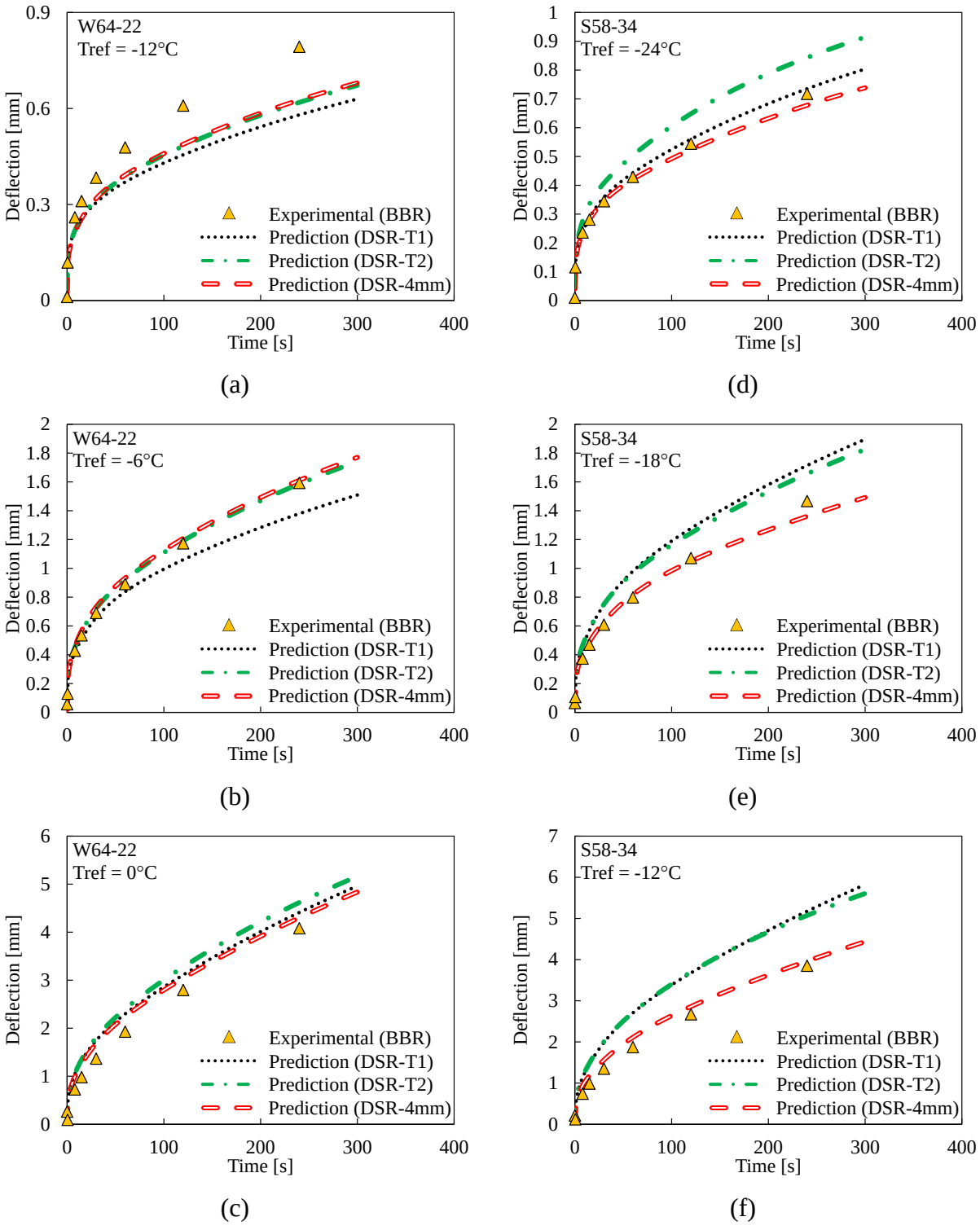

Figure 4.21 DSR beam deflection prediction at different temperatures with a_β = 1.736 for binders: W64-22 at (a) T_{ref} = -12°C (b) T_{ref} = -6°C (c) T_{ref} = 0°C and S58-34 (d) T_{ref} = -24°C (e) T_{ref} = -18°C (f) T_{ref} = -12°C.

Figure 4.22 (a) and (b) compare the DSR predictions with the BBR test results for the creep stiffness $S(t$=60s) and the slope $m(t$=60s), respectively. It can be observed that the shift factor a_β = 1.736 can provide better results for stiffness predictions for all binders compared to the predictions without any hardening adjustment factor (i.e., a_β = 1.0). Figure 4.22 (a) shows that most predictions using the shift factor of 1.736 are close to the line of equality with some binders that still tend to overpredict the stiffness values, which is due to the use of a global adjustment value rather than using binder-case-specific shift factors. Regarding the slope predictions, there was no significant improvement in the predictions by using the adjustment factor. An additional horizontal shifting in the slope values by 0.04 was still necessary for providing the best match with the experimental values as demonstrated in Figure 4.22 (c).

Based on the observed results from the binder dataset included in this study, two steps of shifting are recommended for the prediction: one for the creep compliance, $J(t/a_\beta)$ for predicting the deflection values using a_β = 1.736 in Equation 4.9 and another horizontal shifting particularly for the *m*-value by 0.04.

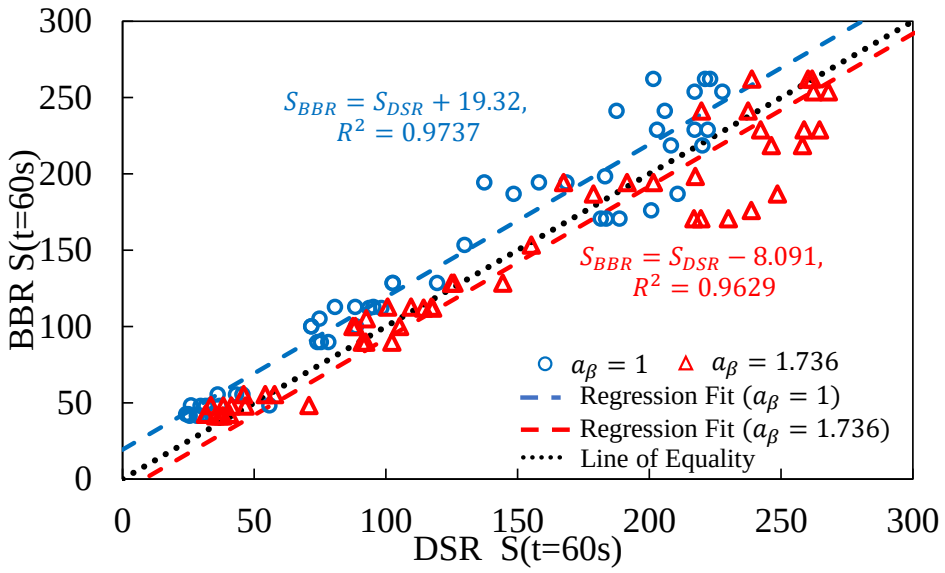

(a)

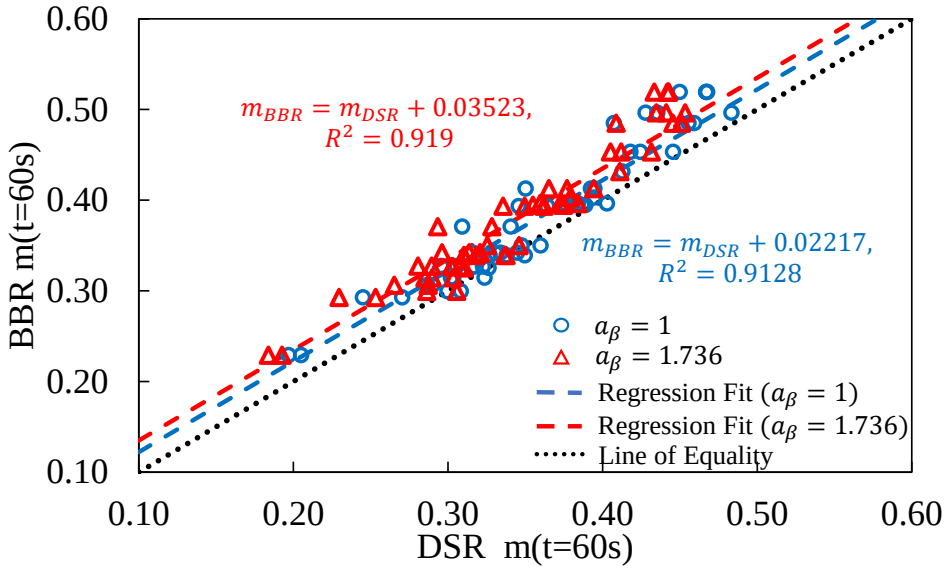

(b)

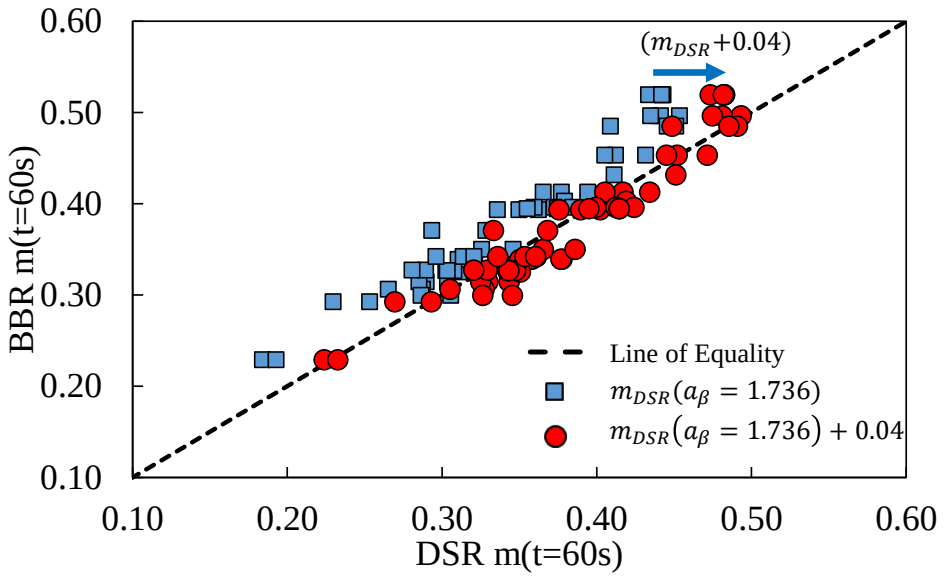

(c)

Figure 4.22 (a) Comparison of the DSR predicted results with experimental BBR results: (a) stiffness *S*(*t*=60s), (b) slope *m*(*t*=60s), (c) additional shifting for *m*-value.

4.5.3 Repeatability analysis

In the previous section, it was shown that differences in measured |*G**| values at low temperatures (between 0°C to -30°C) in various trials resulted in variation of the deflection predictions using Equation (4.9). In order to assess the level of influence how such variations can cause on the predicted values, a repeatability analysis was conducted on sample J58-34 using Equation (4.9) with a_β = 1.736. The choice of the selected binder was random and is assumed that similar results can be obtained with other binders.

For the repeatability analysis, the same DSR testing was conducted a total nine times on a single binder, J58-34. The nine trials were divided into three sets, set-1 consisted of trials T1 and T2 where deliberately more amount of binder was trimmed between the parallel plates, in set-2 consisting of trials T3 to T7, where precise trimming of binder was attempted and set-3 which consists of trials T8 and T9, where less amount of binder was intentionally trimmed. Figure 4.23 (a) shows the |*G**| master curves for each of the trials at a reference temperature T_{ref} = -24°C. It can be observed that difference in sample trimming process can result in a band width of |*G**| values. Using the results, an average and its 95% confidence interval at each reduced frequency was obtained for each set, and results are shown in Figure 4.23(b). It can be seen that the mean of set-1 and set-3 lie outside the 95% confidence interval, which indicate significantly different master curves which are expected due to the less (or more) amount of binder placed between the plates. Figure 4.24 compare the deflection predictions for each set. It presents that the trimming process clearly influences results. Set-1 resulted in 25% under-prediction and set-3 resulted in 40% over-prediction of the stiffness parameter. In case of slope parameter, set-1 resulted in 7% under prediction and set-3 resulted in 2.6% over prediction. Figure 4.25 plots COV values of each DSR set and the corresponding BBR. In general, the variability was greater with DSR compared to BBR. The repeatability of DSR, although it shows a generally satisfactory level, is influenced by trimming and sample preparation process. In particular, the creep stiffness is sensitive because it can be directly affected by the amount of materials between the plates, and the sensitivity will be more pronounced at lower testing temperatures.

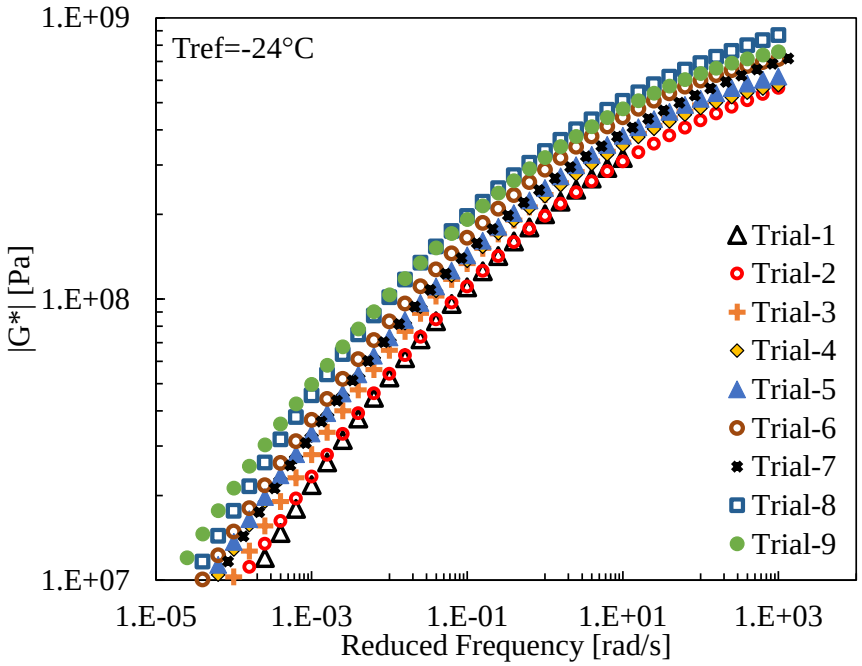

(a)

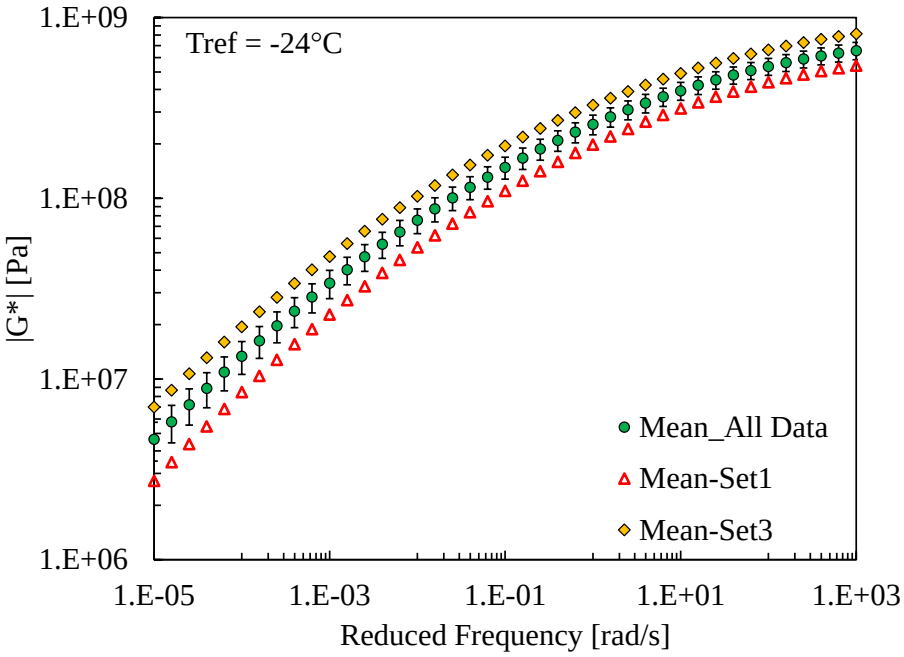

(b)

Figure 4.23 (a) Master curve of |*G**| for J58-34 for trial-1 to trial-9, (b) |*G**| average values of all data with a 95% confidence interval with |*G**| average of set-1 and set-3.

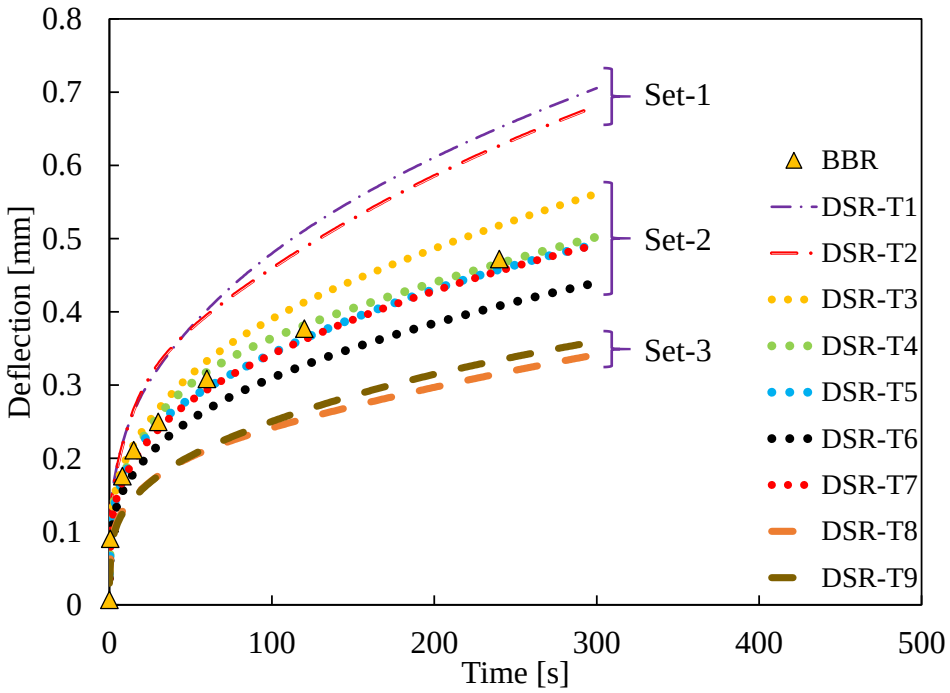

Figure 4.24 Deflection predictions of all nine trials with binder J58-34.

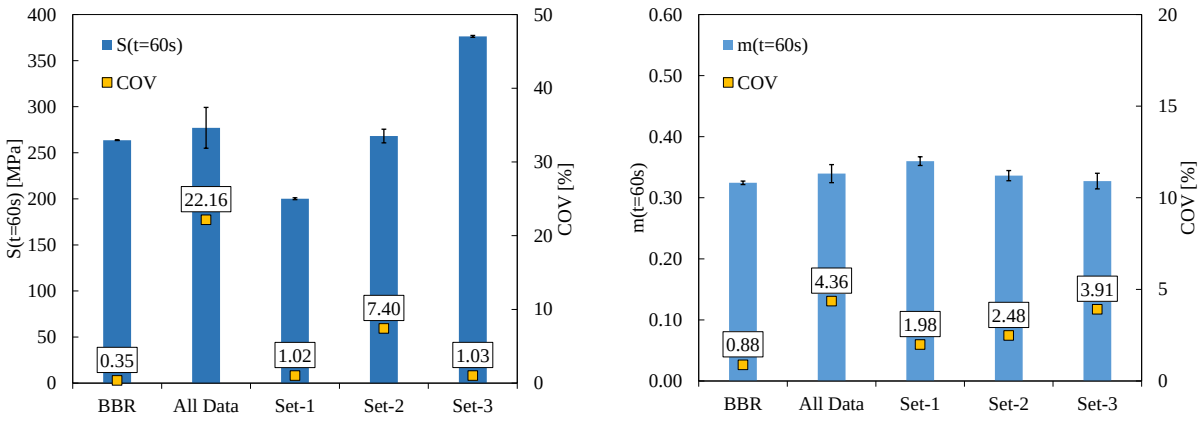

(a) (b)

Figure 4.25 BBR and DSR of binder J58-34: (a) average creep stiffness and corresponding COV, (b) average slope and corresponding COV.

4.5.4 Application of UNL's mechanistic approach to another set of binders

In order to see the feasibility of the UNL's mechanistic approach for predicting the BBR results using DSR test and data, seven binders were additionally selected from NDOT. These binders were tested and graded based on the UNL's mechanistic approach and the results are shown in Figure 4.26 and Figure 4.27. In general, a good match between (BBR) measurements and (DSR) predictions was observed from all binders except V2.

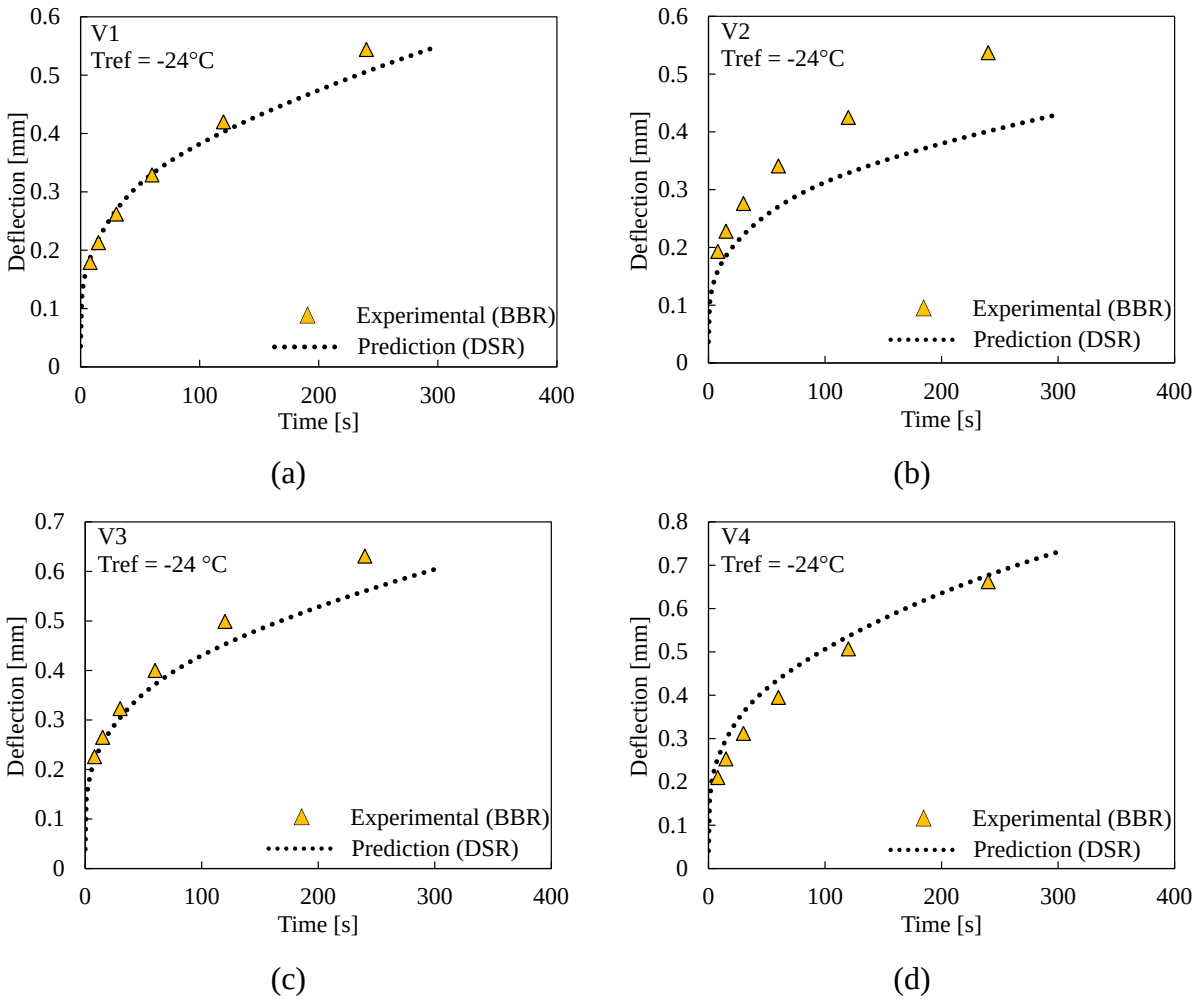

Figure 4.26 Comparison of beam deflections over loading time between the BBR measurements and DSR predictions using the UNL's mechanistic approach: (a) V1, (b) V2, (c) V3, (d) V4.

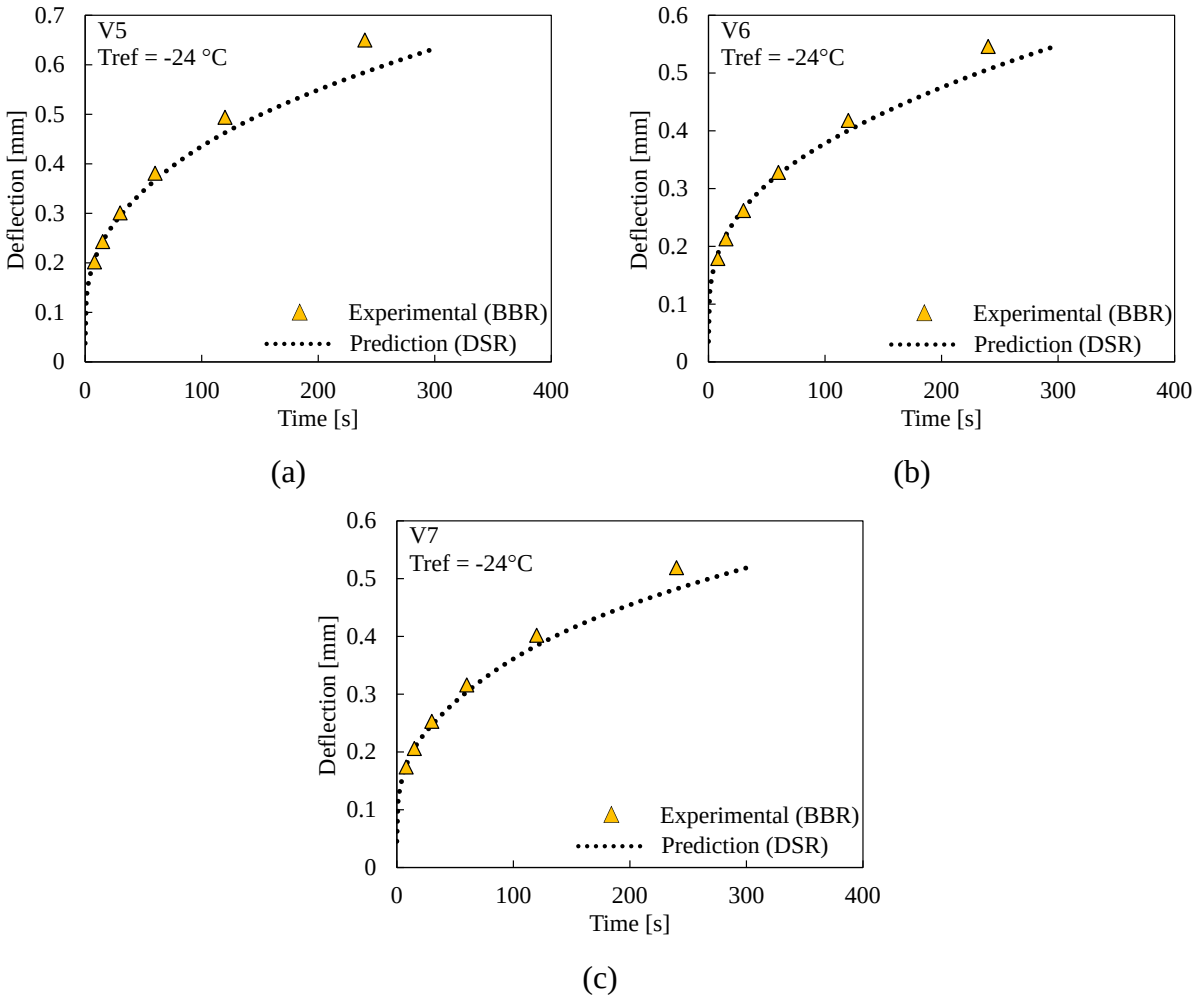

Figure 4.27 Comparison of beam deflections over loading time between the BBR measurements and DSR predictions using the UNL's mechanistic approach: (a) V5, (b) V6, (c) V7.

Table 4.6 shows the two low temperature PG-grading parameters (i.e., $S(t=60s)$ and $m(t=60s)$) comparing the BBR data with the predicted values using the UNL's methodology from the seven binders. It can be seen that the slope predictions were quite promising moreover, for most of the binders the predicted parameters showed an absolute error less than 15% and 6% for stiffness and slope, respectively. The stiffness prediction for the binder V2 was more than 300 MPa and over predicted by at least 33% which resulted in different low PG grading compared to the corresponding BBR grading. It is expected to improve the accuracy with a more precisely identified adjustment factor through a more comprehensive characterization of binders and testing conditions.

Table 4.6 Comparison of PG grading for seven binders using Equation 4.9 and a_β = 1.736

Binder	Results from BBR		Results from DSR		Absolute % Error		Same Grading
	$S(t=60s)$	$m(t=60s)$	$S(t=60s)$	$m(t=60s)$	$S(t=60s)$	$m(t=60s)$	
V1	246	0.34	261.45	0.33	6.28	2.94	YES
V2	238	0.311	318.61	0.32	33.87	2.89	NO
V3	205	0.315	233.86	0.33	14.08	4.76	YES
V4	206	0.35	197.07	0.33	4.33	5.71	YES
V5	212	0.355	237.49	0.35	12.02	1.41	YES
V6	250	0.34	263.84	0.34	5.54	0.00	YES
V7	256	0.336	284.68	0.34	11.20	1.19	YES

Chapter 5. Summary and Conclusions

This study investigated alternative testing-analysis methods using the DSR to determine low temperature asphalt binder properties that have conventionally been measured by the BBR. Toward that end, twelve different binders from four sources satisfying three different PG grading criterion common in Nebraska were selected. The binder samples were tested in the frequency domain in a wide range of temperatures under PAV-aged conditions using DSR. The 8-mm parallel plate geometry was primarily employed for the testing, while four binders were randomly selected and tested using the 4-mm parallel plate to investigate the influence of geometry on the results. BBR experiments were also performed as a parallel for each binder. Three methods were used to analyze and compare the data from the two different experiments (i.e., DSR and BBR) where each method utilized a different scheme for converting the frequency domain results to time domain data to compare with the BBR results. The three methods were: (1) Western Research Institute's (WRI) methodology; (2) NCHRP methodology; and (3) UNL's mechanistic approach. The following conclusions can be drawn based on the test and analysis results:

- It was observed that the WRI methodology works well but is dependent on the binder dataset used. With the current binder set in this study, the cutoff values were $G(t=60s) < 85.5$ MPa and $m(t=60s) > 0.287$ which are different from values reported in the literature.

- The NCHRP method is promising and provided a good linear correlation between the DSR predicted stiffness/slope values and the corresponding experimental BBR values. Good prediction was observed for the creep stiffness, whereas the slope values were always underpredicted. Also, the NCHRP method is considered efficient when grading PG 64-22 or higher-graded binders because one can easily use the method at temperatures above 0°C to obtain a reasonable estimate of stiffness and slope without performing any further experiments below freezing temperature.

- In the UNL's mechanistic approach, it was observed that the Prony series representation of the binder properties is mechanically sound and rigorous. It can be used effectively to predict the BBR results. It was also observed that the sample preparation was very important to produce a repeatable and reliable test results and corresponding predictions.

- In the UNL's mechanistic approach, several intrinsic aspects such as the effects of cooling media and physical hardening of binder at different temperature can be potentially addressed by introducing an adjustment factor. The adjustment factor was observed to be binder specific and temperature dependent, however a global adjustment factor of a_β = 1.736 obtained from the binder data set in this study could provide a satisfactory level of prediction for creep stiffness. An additional horizontal shifting of 0.04 was necessary to match the slope (*m*-value) predictions.

- Overall, the use of DSR as an alternative testing-analysis method to characterize binder low temperature properties looks quite feasible; however, its actual implementation into practice requires a more careful investigation. More binders in different types and test results obtained from various testing conditions are necessary to make more definite conclusions. Nonetheless, the DSR method can be used as (at least) a screening tool to judge whether a binder given requires the entire process of BBR testing or not, which will clearly improve testing efficiency of many state Departments of Transportation including the NDOT.

References

1. Isacsson U, Zeng H. Cracking of asphalt at low temperature as related to bitumen rheology. Journal of materials science. 1998;33(8):2165-70.
2. Anderson DA, Christensen DW, Bahia HU, Dongre R, Sharma M, Antle CE, et al. Binder characterization and evaluation, volume 3: Physical characterization. Strategic Highway Research Program, National Research Council, Report No SHRP-A-369. 1994.
3. Fabb T, editor The influence of mix composition, binder properties and cooling rate on asphalt cracking at low temperatures. Association of Asphalt Paving Technologists Proc; 1974.
4. Lesueur D, Gerard JF, Claudy P, Letoffe JM, Planche JP, Martin D. A structure-related model to describe asphalt linear viscoelasticity. Journal of Rheology. 1996;40(5):813-36.
5. Edwards Y, Tasdemir Y, Isacsson U. Rheological effects of commercial waxes and polyphosphoric acid in bitumen 160/220—low temperature performance. Fuel. 2006;85(7-8):989-97.
6. Lu X, Isacsson U. Rheological characterization of styrene-butadiene-styrene copolymer modified bitumens. Construction and Building Materials. 1997;11(1):23-32.
7. Lu X, Isacsson U. Chemical and rheological evaluation of ageing properties of SBS polymer modified bitumens. Fuel. 1998;77(9-10):961-72.
8. Lu X, Isacsson U, Ekblad J. Low-temperature properties of styrene–butadiene–styrene polymer modified bitumens. Construction and Building Materials. 1998;12(8):405-14.
9. Lu X, Isacsson U. Artificial aging of polymer modified bitumens. Journal of applied polymer science. 2000;76(12):1811-24.
10. Lu X, Isacsson U. Modification of road bitumens with thermoplastic polymers. Polymer testing. 2000;20(1):77-86.
11. Lu X, Isacsson U. Effect of binder rheology on the low-temperature cracking of asphalt mixtures. Road Materials and Pavement Design. 2001;2(1):29-47.
12. Sui C, Farrar M, Tuminello W, Turner T. New technique for measuring low-temperature properties of asphalt binders with small amounts of material. Transportation Research Record: Journal of the Transportation Research Board. 2010(2179):23-8.
13. Sui C, Farrar M, Harnsberger P, Tuminello W, Turner T. New low-temperature performance-grading method: Using 4-mm parallel plates on a dynamic shear rheometer. Transportation Research Record: Journal of the Transportation Research Board. 2011(2207):43-8.
14. Farrar M, Sui C, Salmans S, Qin Q. Determining the low temperature rheological properties of asphalt binder using a dynamic shear rheometer (DSR). Technical White Paper FP08 Prepared by Western Research Institute for the Federal Highway Administration. Contract No DTFH61-07-D-00005, Fundamental Properties of Asphalts and Modified Asphalts, III. 2015.
15. Farrar M, Grimes RW, Sui C, Planche J-P, Huang S-C, Turner TF, et al., editors. Thin film oxidative aging and low temperature performance grading using small plate dynamic shear rheometry: an alternative to standard rtfo, pav, and bbr. Proceedings of the 5th Eurasphalt and Eurobitumen Congress; 2012 June 13-15; Istanbul, Turkey.
16. Behnia B, Buttlar W, Reis H. Evaluation of Low-Temperature Cracking Performance of Asphalt Pavements Using Acoustic Emission: A Review. Applied Sciences. 2018;8(2):306.

17. Velasquez R, Bahia H. Critical factors affecting thermal cracking of asphalt pavements: towards a comprehensive specification. Road Materials and Pavement Design. 2013;14(sup1):187-200.
18. Stimilli A, Virgili A, Canestrari F, Bahia HU. Estimation of low-temperature performance of recycled asphalt mixtures through relaxation modulus analysis. Cold Regions Science and Technology. 2017;133:36-45.
19. Marasteanu MO, Cannone Falchetto A. Review of experimental characterisation and modelling of asphalt binders at low temperature. International Journal of Pavement Engineering. 2018;19(3):279-91.
20. Dongré R, D'Angelo J, McMahon S. Development of superpave direct tension test device. Transportation Research Record: Journal of the Transportation Research Board. 1997(1586):32-9.
21. Basu A, Marasteanu M, Hesp S. Time-temperature superposition and physical hardening effects in low-temperature asphalt binder grading. Transportation Research Record: Journal of the Transportation Research Board. 2003(1829):1-7.
22. Premkumar L, Chehab G, Solaimanian M. Evaluation of Low-Temperature Properties of Asphalt Binders and Mixtures. Transportation Research Record: Journal of the Transportation Research Board. 2013(2370):102-8.
23. Velasquez R, Tabatabaee H, Puchalski S, Bahia H, editors. The role of asphalt binder fracture properties in thermal cracking performance of mixtures and pavements. Proceedings of the 57th Annual Conference of the Canadian Technical Asphalt Association (CTAA), Vancouver, British Columbia; 2012.
24. Lee NK, Hesp SA. Low-temperature fracture toughness of polyethylene-modified asphalt binders. Transportation Research Record. 1994(1436).
25. Hoare T, Hesp S. Low-temperature fracture testing of asphalt binders: regular and modified systems. Transportation Research Record: Journal of the Transportation Research Board. 2000(1728):36-42.
26. Hesp S. An improved low-temperature asphalt binder specification method. Final Report, Queen's University, Ontario. 2004.
27. Chailleux E, Hamon D, Mouillet V, editors. Determination of the low temperature bitumen cracking properties: fracture mechanics principle applied to a three points bending test using a non homogeneous geometry. 10TH INTERNATIONAL CONFERENCE ON ASPHALT PAVEMENTS-AUGUST 12 TO 17, 2006, QUEBEC CITY, CANADA; 2006.
28. Velasquez R, Tabatabaee H, Bahia H. Low temperature cracking characterization of asphalt binders by means of the single-edge notch bending (SENB) test. Asphalt Paving Technology-Proceedings Association of Asphalt Technologists. 2011;80:583.
29. Marasteanu M, Zofka A, Turos M, Li X, Velasquez R, Li X, et al. Investigation of low temperature cracking in asphalt pavements national pooled fund study 776. 2007.
30. Andriescu A, Hesp SA, Youtcheff JS. Essential and plastic works of ductile fracture in asphalt binders. Transportation Research Record. 2004;1875(1):1-7.
31. Dongre R, Sharma M, Anderson D. Development of fracture criterion for asphalt mixes at low temperatures. Transportation Research Record. 1989;1228:94-105.
32. Zofka A, Marasteanu M. Development of double edge notched tension (DENT) test for asphalt binders. Journal of Testing and Evaluation. 2006;35(3):259-65.

33. Hou Y, Wang L, Yue P, Sun W. Fracture failure in crack interaction of asphalt binder by using a phase field approach. Materials and Structures. 2015;48(9):2997-3008.
34. Kim S-S, Wysong Z, Kovach J. Low-temperature thermal cracking of asphalt binder by asphalt binder cracking device. Transportation Research Record: Journal of the Transportation Research Board. 2006(1962):28-35.
35. Kim S-S. Direct measurement of asphalt binder thermal cracking. Journal of Materials in Civil Engineering. 2005;17(6):632-9.
36. Kim S-S. Development of an Asphalt Binder Cracking Device. 2007.
37. Jiao Y, Fu L, Shan W, Liu S. Damage fracture characterization of pervious asphalt considering temperature effect based on acoustic emission parameters. Engineering Fracture Mechanics. 2018.
38. Tabatabaee HA, Velasquez R, Bahia HU. Predicting low temperature physical hardening in asphalt binders. Construction and Building Materials. 2012;34:162-9.
39. Baglieri O, Dalmazzo D, Barazia M, Tabatabaee HA, Bahia HU. Influence of physical hardening on the low-temperature properties of bitumen and asphalt mixtures. Procedia-Social and Behavioral Sciences. 2012;53:504-13.
40. Laukkanen O-V, Winter HH, Soenen H, Seppälä J. Systematic broadening of the viscoelastic and calorimetric glass transitions in complex glass-forming liquids. Journal of Non-Crystalline Solids. 2018;483:10-7.
41. Laukkanen O-V, Winter HH, Seppälä J. Characterization of physical aging by time-resolved rheometry: fundamentals and application to bituminous binders. Rheologica Acta. 2018;57(11):745-56.
42. Lu X, Uhlback P, Soenen H. Investigation of bitumen low temperature properties using a dynamic shear rheometer with 4 mm parallel plates. International Journal of Pavement Research and Technology. 2017;10(1):15-22.
43. Laukkanen O-V. Small-diameter parallel plate rheometry: a simple technique for measuring rheological properties of glass-forming liquids in shear. Rheologica Acta. 2017;56(7-8):661-71.
44. Laukkanen O-V. Low-temperature rheology of bitumen and its relationship with chemical and thermal properties [Master's Thesis]. Espoo, Finland: Aalto University; 2015.
45. Laukkanen O-V, Soenen H, Winter HH, Seppälä J. Low-temperature rheological and morphological characterization of SBS modified bitumen. Construction and Building Materials. 2018;179:348-59.
46. Carret J-C, Falchetto AC, Marasteanu MO, Di Benedetto H, Wistuba MP, Sauzeat C. Comparison of rheological parameters of asphalt binders obtained from bending beam rheometer and dynamic shear rheometer at low temperatures. Road Materials and Pavement Design. 2015;16(sup1):211-27.
47. Riccardi C, Cannone Falchetto A, Wang D, Wistuba MP. Effect of cooling medium on low-temperature properties of asphalt binder. Road Materials and Pavement Design. 2017;18(sup4):234-55.
48. Hutcheson S, McKenna G. The measurement of mechanical properties of glycerol, m-toluidine, and sucrose benzoate under consideration of corrected rheometer compliance: an in-depth study and review. The Journal of chemical physics. 2008;129(7):074502.
49. Liu C-Y, Yao M, Garritano RG, Franck AJ, Bailly C. Instrument compliance effects revisited: linear viscoelastic measurements. Rheologica acta. 2011;50(5-6):537.

50. Schröter K, Hutcheson S, Shi X, Mandanici A, McKenna G. Dynamic shear modulus of glycerol: Corrections due to instrument compliance. The Journal of chemical physics. 2006;125(21):214507.
51. Christensen R. Theory of viscoelasticity: an introduction: Elsevier; 2012.
52. Park S, Schapery R. Methods of interconversion between linear viscoelastic material functions. Part I—A numerical method based on Prony series. International Journal of Solids and Structures. 1999;36(11):1653-75.
53. Ghorban Ebrahimi M, Saleh M, Gonzalez MAM. Interconversion between viscoelastic functions using the Tikhonov regularisation method and its comparison with approximate techniques. Road Materials and Pavement Design. 2014;15(4):820-40.